Arabian Journal of Chemistry (2023) **16**, 105024

King Saud University

Arabian Journal of Chemistry

www.ksu.edu.sa
www.sciencedirect.com

REVIEW ARTICLE

Review of different CdS/TiO_2 and WO_3/ g-C_3N_4 composite based photocatalyst for hydrogen production

Zain Ashfaq [a,*], Tahir Iqbal [a], Hussnain Ali [b], Sayed M. Eldin [c], Mohammad Mahtab Alam [d], F.F. Al-Harbi [e], Mubashar Arshad [b], Ahmed M. Galal [f,g]

[a] *Department of Physics, Faculty of Sciences, University of Gujrat, Hafiz Hayat Campus, Gujrat 50700, Pakistan*
[b] *Department of Chemical Engineering, University of Engineering and Technology Faisalabad Campus, Faisalabad 38000, Pakistan*
[c] *Center of Research, Faculty of Engineering, Future University in Egypt New Cairo, 11835, Egypt*
[d] *Department of Basic Medical Sciences, College of Applied Medical Science, King Khalid University, Abha 61421, Saudi Arabia*
[e] *Department of Physics, College of Science, Princess Nourah bint Abdulrahman University, P.O. Box 84428, Riyadh 11671, Saudi Arabia*
[f] *Department of Mechanical Engineering, College of Engineering in Wadi Alddawasir, Prince Sattam bin Abdulaziz University, Saudi Arabia*
[g] *Production Engineering and Mechanical Design Department, Faculty of Engineering, Mansoura University, P.O. 35516, Mansoura, Egypt*

Received 9 March 2023; revised 16 May 2023; accepted 17 May 2023
Available online 30 May 2023

KEYWORDS

Photocatalyst activity;
Semiconductor photocatalyst;
Hydrogen production;
Water splitting;
Cadmium Sulfide (CdS) and Tungsten trioxide (WO_3);
Titanium dioxide (TiO_2) and Graphite Carbon Nitride (gC_3N_4)

Abstract The production of hydrogen from water is one of the best sustainable energy resources to fulfill the increasing energy deficiency of the world. As most of the available energy resources are harmful in one way or another as nuclear waste is dangerous for human life and burning fossil fuels caused the production of carbon, nitrogen, and Sulphur oxides which increases global warming as well as air pollution. The earth is almost 70% consist of water so that there is need to use this water in efficient way to produce hydrogen as it is more sustainable energy resource and environment friendly. This is an emerging field for researchers and they trying to find the best photocatalyst for hydrogen production. The motivation of this study is to provide improved mechanism for hydrogen production because the developing countries like Pakistan faced serious energy crisis and available energy resources in these countries are the fossil fuels mostly which are not

* Corresponding author.
E-mail address: zainashfaq147@gmail.com (Z. Ashfaq).
Peer review under responsibility of King Saud University. Production and hosting by Elsevier.

Production and hosting by Elsevier

https://doi.org/10.1016/j.arabjc.2023.105024

environmentally friendly creating chaos of global warming. The background of this study shows that researcher used doped, composite, and many other different techniques to enhance its efficiency. For the last decade, researchers mainly focused on the doped photocatalyst. In recent decade researcher shifted to composite based photocatalysts. The hypothetical question arises in this study weather these composite useful to improve efficiency of hydrogen production by using photocatalyst method? This review paper especially focuses on different composite photocatalysts for hydrogen production. The composites of Cadmium Sulfite/Titanium dioxide (CdS/TiO_2) and Tungsten trioxide/graphite Carbon nitride (WO_3/ g-C_3N_4) have been the main area of interest in this review due to their immense use in research to produce hydrogen. This study will also help to understand the mechanism of the production of hydrogen through water splitting and organic compounds. The study also elaborates on the zigzag (Z) and step (S) schemes used for the photocatalytic activity of composites. Present work showed that composite photocatalyst are better and increased efficiency of hydrogen production because active sites of surface increased. This review will be helpful for new apprentices in this field to understand the basic mechanism, helpful for industrialists and experts to decide which composite photocatalyst is best according to their interests.

1. Introduction

Immense use of fossil fuels causes worse environmental issues. So, it's now need for the world to find sustainable energy resources. With the passage of time researchers shift the environmentally friendly energy resources method in which solar energy. But one of the best sustainable energy resources is hydrogen production through water splitting by using the photocatalytic method which is environment friendly and cost-effective method. The technoeconomic analysis showed that 1 kg hydrogen production through photocatalyst cost almost 9$ and electrolysis method cost 18$ (Hermesmann and Müller, 2022, Montoya et al., 2017, Chu et al., 2017). Mostly photocatalysts based on semiconductors are reported by researchers due to their cleanliness and simplicity. This phenomenon was explored by Fujishima and Honda (Anpo et al., 1997). Many synthesized photocatalysts are used to obtain stability and higher efficiency, including nitrides of carbon (Huang et al., 2021), polymers (Ajma et al., 2022), carbides (Soni et al., 2022), metal oxides (Nunes et al., 2021), sulfides (Sudhaik et al., 2022), organic complex metals (Younis et al., 2020), and many others (Nguyen et al., 2015, Hu et al., 2015, Janaky et al., 2012, Wang et al., 2009). The semiconductor material lies between the conductor and the insulator. They have a band gap of up to 1ev usually. When a photon target on semiconductor molecule the electrons of molecule absorb the energy and jumps from valence to the conduction band. During this mechanism electron at the conduction band used for reduction and hole charge carriers produced at the valence band used for oxidation reaction to increase the efficiency of this photocatalytic process recombination of electron and hole must be prevented as much as possible.

Titanium dioxide (TiO_2) is a frequently reported photocatalysts semiconductor used for the production of hydrogen because TiO_2 has several advantages inert biologically and chemically, simple production and use, cost-effective, environmentally friendly, and stable but its disadvantage is activated in the UV region, not the ultraviolet region (Akpan and Hameed, 2009).

There are thousands of articles published in the last 20 years on TiO_2-based photocatalysts as shown in Fig. 1.

Another mostly used semiconductor photocatalyst for hydrogen production recently tungsten trioxide (WO_3) attracts the researchers due to its high stability, sharp band edges, non-toxicity, long life, low cost, easy access and activation in the visible region at a wavelength of 470 nm. But, WO_3 has a few limitations as well. Firstly, WO_3 has low specific area. Secondly, a less visible light response of more than 470 nm wavelength. Thirdly due to the low conduction band many reactions do not occur one of them oxygen reduction for a single electron and fourthly it has fast electro-hole pair recombination rate (Liao et al., 2021).

There are thousands of articles published in the last 20 years on WO_3-based photocatalysts as shown in Fig. 2.

Another interesting photocatalyst semiconductor used for hydrogen production is cadmium sulfite (CdS) due to its great response in the visible region, narrow bandgap, and good conduction band for protons reduction.

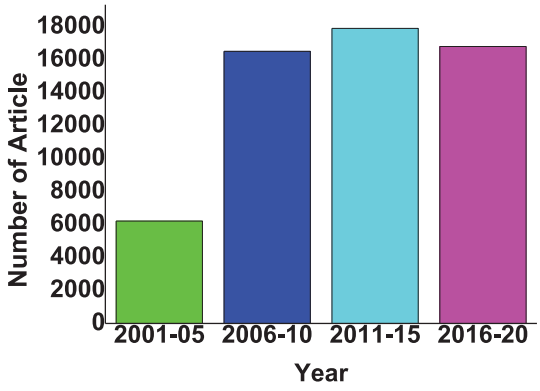

Fig. 1 TiO_2 based photocatalyst reported in last two decades with the gap of 5 years from 2001 to 2020 from google scholar (Scholar, 2001–2020).

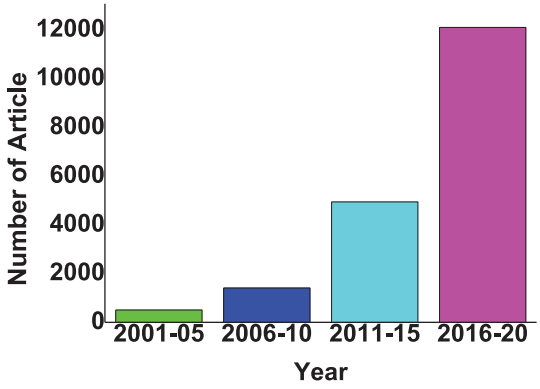

Fig. 2 WO_3 based photocatalyst reported in last two decades with the gap of 5 years from 2001 to 2020 from google scholar (Scholar, 2001-2020c).

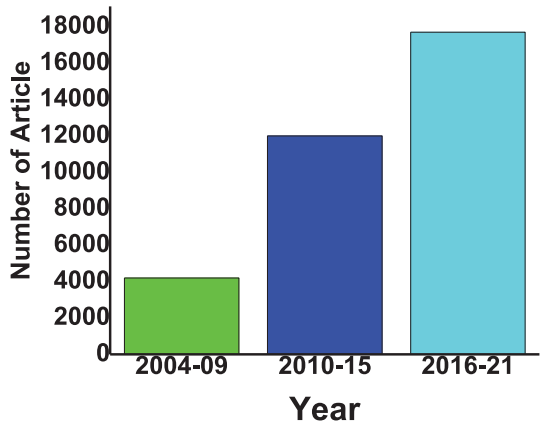

Fig. 3 CdS based photocatalyst reported in last two decades in with the gap of 5 years from 2004 to 2021 from google scholar (Scholar, 2001-2020a).

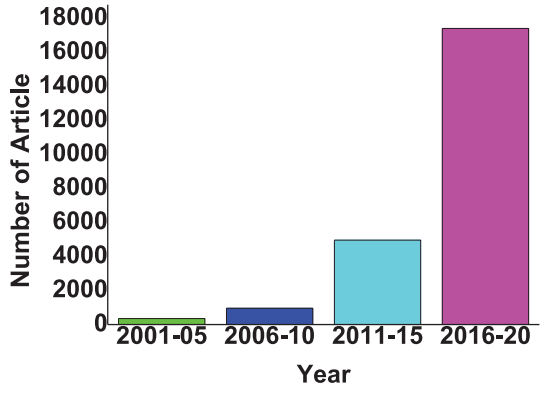

Fig. 4 g C_3N_4 based photocatalyst reported in last two decades with the gap of 5 years from 2001 to 2020 from google scholar (Scholar, 2001-2020b).

CdS has some shortcomings occur such as CdS is alterable, instable and cannot be useable for the long terms and Its efficiency decreased with passage of time (Cheng et al., 2018).

There are thousands of articles published in the last 20 years on CdS-based photocatalysts as shown in Fig. 3.

Graphite Carbon nitride (g C_3N_4) based photocatalyst for hydrogen production gain the attraction of researchers due to their high chemical stability, easy availability as g C_3N_4 is the most earthbound elements.

Despite all the interesting features, it has a few drawbacks like lacking solar light absorption, fast electron-hole pair recombination, and less surface area (Nasir et al., 2019a).

There are thousands of articles published in the last 20 years on g C_3N_4-based photocatalyst as shown in Fig. 4.

Immense of research articles published by the researcher on TiO_2, CdS, g C_3N_4, and WO_3-based photocatalysts in the last two decades (Akpan and Hameed, 2009, Cheng et al., 2018, Munawar et al., 2022, Dutta et al., 2021, Liao et al., 2021, Luo et al., 2017, Chen et al., 2020, Liu et al., 2021, Yang et al., 2021, Wen et al., 2017). Recently in the last seven years, researchers shifted their interest towards the composite of this semiconductor photocatalyst for the production of hydrogen to deal with the drawback of the above-discussed semiconductor-based photocatalyst and comparison shown in Table 1.

The main purpose of this study is to focus especially on the discussion of different WO_3 composites, CdS composites, TiO_2 composites, and g C_3N_4 composites for hydrogen production. Because the research gap found that no review article has been published on photocatalyst based composite for hydrogen production and there is need for research to focus on two-dimension (2D) composites for further study in this domain. Then after the study of different composite provide the reader with a detailed comparison of different composites. This study will also focus on the crone and prone of different composite. In the end, this study will give the future aspects, challenges, and limitations in using the different composite photocatalysts for the production of hydrogen. This study also studies the brief mechanism of water splitting and organic compounds for the production of hydrogen. Further, Schemes used by composites for photocatalytic are also discussed briefly. This study will help the new researcher to understand the mechanism and it will also help the expert to decide which composite is best for further study.

2. Composites-based photocatalysts for hydrogen (H_2) evolution

Hydrogen production from water splitting by using photocatalyst semiconductor is cost-effective, sustainable and pollution-free energy resource. Even many researchers tried to take the best outcomes but few restrictions like nonstable, less activation in the visible region, and fast recombination of electron-hole pair. For solving this issue composite (Elmacı et al., 2019, Elmaci et al., 2015, Elmacı et al., 2016, Elmacı et al., 2020) of two catalysts help in modifying the valence and conduction band by enhancing reduction and oxidation and is also helpful in activation in the visible region. The different composites are reported by researchers some of them illustrated below discussion (Weng and Xu, 2015, Li et al., 2020, An and Jimmy, 2011). There are thousands of articles published in this era on composite for hydrogen production (Ghouri et al., 2021, Mao et al., 2022, Guan et al., 2004, Lee, 2005) as shown in Fig. 5.

Table 1 Comparison of different semiconductor Photocatalyst.

Photocatalyst semiconductor	Band Gap	Advantages	Limitation	
CDs	2.42 eV	Activation in visible Narrow band gap	Unstable Not useable for long term	(Cheng et al., 2018)
TiO_2	3.2 eV	Stable Simple Production	No activation in the visible range	(Akpan and Hameed, 2009)
WO_3	2.5 eV	Stable Activation in visible	Low conduction band Fast Recombination	(Liao et al., 2021)
g C_3N_4	2.7 eV	Stable Easily available	Low surface area Fast Recombination	(Nasir et al., 2019b)

3. CdS and TiO_2 composite

The bandgap energy of CdS 2.42 eV is smaller and makes it worthy to use under visible light for the decomposition of water through the photocatalyst process. But it has a fast recombination rate of electron-hole pair which make it less efficient for photocatalyst (Husseina et al., 2022). On the contrary, TiO_2 has good electron-hole pair recombination which makes it more efficient for photocatalyst but it has a band gap energy of 3.42 eV which make it disreputable for visible region (Doubi et al., 2022). The researcher started to work on CdS/TiO_2 composite to overcome the photocatalytic barrier of TiO_2 and CdS for the evolution of hydrogen. The composite improved the recombination rate and, in some cases, work in near-visible regions successfully from the range of 420–550 nm. In different sizes (nano bulk, nano, quantum dot) (Doubi et al., 2022) and with different preparation methods (hydrothermal, precipitation, sol–gel) CdS/TiO_2 composites photocatalysts reported by the researcher for the production of hydrogen by different substances (air, water, hydrogen sulfide) (Wang et al., 2022).

In the last decade's lot of publications reported using composite Cds/TiO_2 for hydrogen evolution (Jiang et al., 2017, Lian et al., 2015, Khatamian et al., 2014, Jang et al., 2007b) as shown in Fig. 6.

3.1. CdS and TiO_2 nanocomposite treated with $TiCl_4$

The first CdS and TiO_2 composite was reported by won-wook so et al in 2003 at the nano level with a treated film of $TiCl_4$. won-wook so et al prepared nano-size CdS and TiO_2 solution mixed by using the mole ratio. The further hydrothermal method was used for 12 h at 120–240-degree Celsius (C) temperature. In this way composite of CdS and TiO_2 was prepared and $TiCl_4$ was annealed for 30 min at 400C temperature to obtain the crystalline phase of the composite. By using XRD, SEM, and UV techniques nano composite characteristics and structure were studied (So et al., 2004). Finally, the effect of composite photocatalyst check on the photoreactor as shown in Fig. 7.

The structure and characteristics of the composite treated with $TiCl_4$ illustrates by studying the obtained results from XRD and SEM shown in Fig. 8.

On the base of $TiCl_4$ treated TiO_2/CdS composite production of hydrogen with the time shown in Fig. 9.

The result showed that the production of hydrogen increased with time as photocurrent increased, photocatalytic activity enhanced, and optimum production obtain at a mole ratio of 0.8.

3.2. CdS and TiO_2 nano bulk composite (NBC)

Although there are many limitations in the production of hydrogen but high production of H_2 and the removal of hydrogen sulfite (H_2S) observed by using the composite photocatalyst CdS (bulk)/TiO_2 in the presence of water and 0.1 M Na_2S + 0.02 M Na_2SO_3. The hydrogen is produced from H_2S when H_2S dissolve in alkaline water solution where H_2S reacts with hydroxyl ion (OH^-). Then water forms and by reduction or addition of electron with water molecules it produced hydrogen. In this process hydrogen separated from sulfide. The reaction of this process is shown below. In this process, water is also involved and contributes to the production of hydrogen (Jang et al., 2007a, Jang et al., 2006).

$$H_2S + 2OH^- \rightarrow S^{-2} + 2H_2O$$

$$2e^- + 2H_2O \rightarrow H_2 + 2OH^-$$

$$S^{-2} \rightarrow S + 2e^-$$

During this process production of hydrogen with the passage of time and the dissolution of H_2S in different electrolytes are shown in Fig. 10.

The hydrogen (H_2) production model for CdS bulk with nano sized TiO_2 composite shown in Fig. 11 from H_2S and Fig. 12 from 0.1 M Na_2S + 0.02 M Na_2SO_3 (Jang et al., 2006, Jang et al., 2007a).

In the above models of CdS generated photoelectrons collected by active sites of TiO_2 which provide more time for electron-hole pair recombination increase and make the photocatalyst process more efficient.

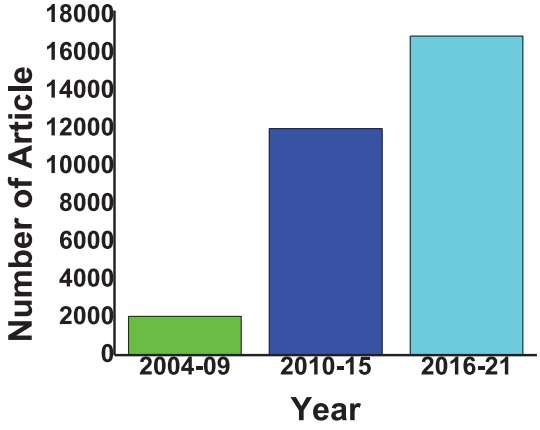

Fig. 5 Publication in last two decades composites based photocatalysts hydrogen evolution with the gap of 5 years from 2004 to 2021 from google scholar (Scholar, 2001-2022a).

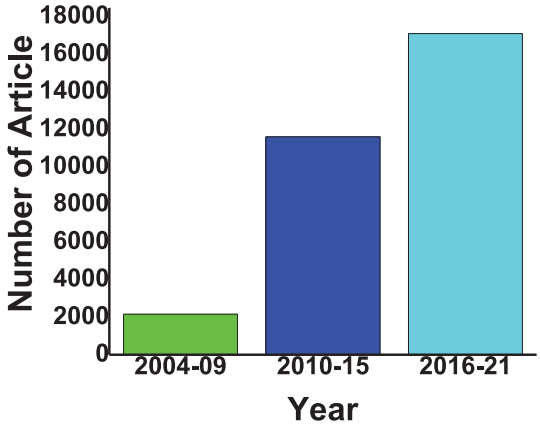

Fig. 6 CdS, TiO_2 composite based photocatalyst reported in last two decades with the gap of 5 years from 2004 to 2021 from google scholar (Scholar, 2022b).

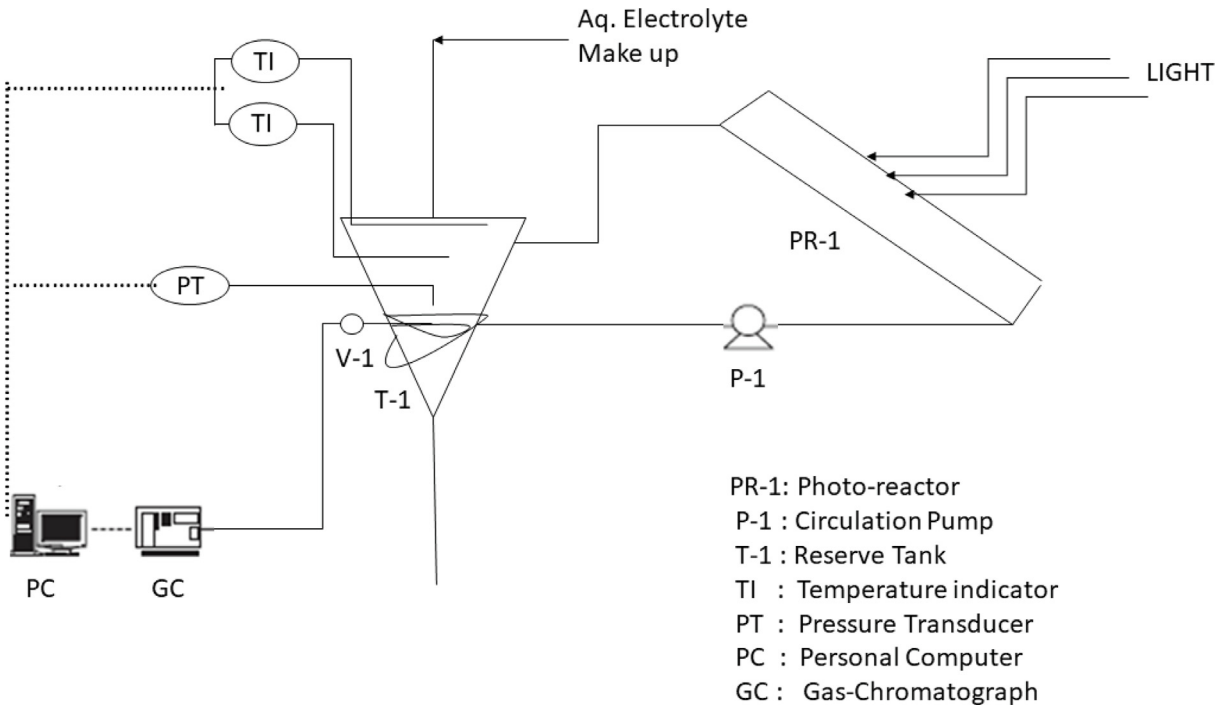

Fig. 7 Photoreactor used to study consist of photo reactor, circulation pump, reserve tank, temperature indicator, pressure transduce, personal computer and gas chromatograph (So et al., 2004).

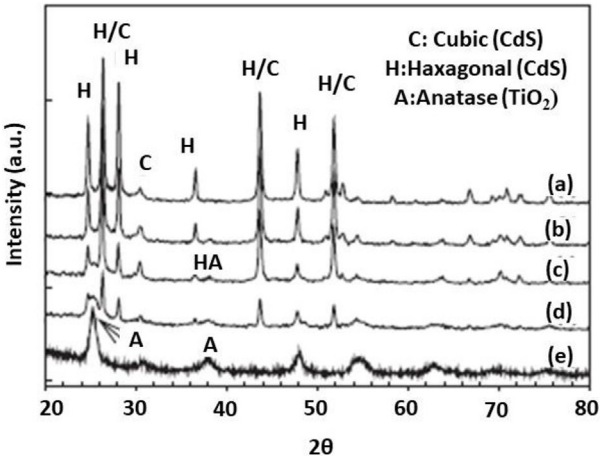

Fig. 8 XRD at mole ratio $TiCl_4$ with composite of CdS/TiO_2 at (a)0 (b)0.2 (c) 0.5 (d) 0.8 (e) 1 here A represents anatase of TiO_2, H hexagonal of CdS and C cubic of CdS (So et al., 2004).

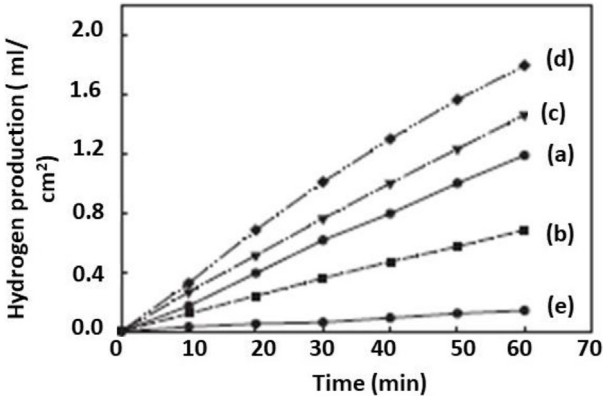

Fig. 9 The figure showed rate of hydrogen (H_2) production in ml/cm^2 in time (min) for CdS/TiO_2 composite particulate prepared with $TiCl_4$ treatment at a mole ratio of (a)0 (b)0.2 (c) 0.5 (d) 0.8 (e) 1 (So et al., 2004).

3.3. Platinum in platinized CdS/TiO_2 composite photocatalysts

Platinization of photocatalyst composite CdS/TiO_2 has been done by using different means like wet impregnation (WI), photo deposition (PD), and chemical reduction (CR) for the production of hydrogen in the visible region. For this purpose, platinum (Pt) in a metallic state is planted on the composite. On the other hand, the photocatalyst of WI and PD consists of electron-deficient Pt. In WI Pt-Ti is formed to fill this deficiency, in this way the electron-hole pairs recombination required more time due to two electrons deficient photocatalysts and makes hydrogen production more efficient from water.

The Pt becomes much more important because of extra higher and lower states created due to WI, PD, and CR processes which make the CdS/TiO_2 composite photocatalysts more efficient. The activity of this model, operation of composite and production of hydrogen with time by using PD, WI, and CR in platinum is shown in Fig. 13 (Jang et al.,

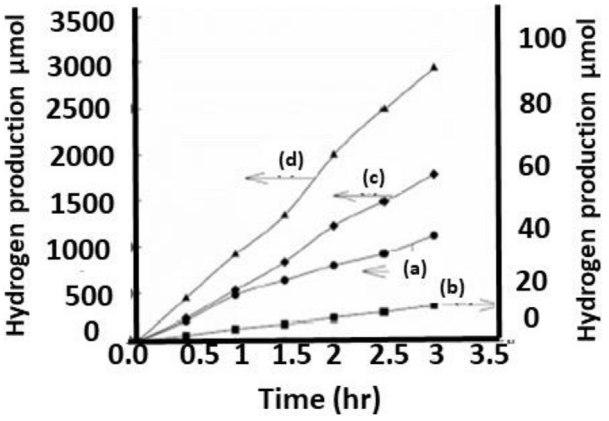

Fig. 10 The rate of hydrogen production in time (hr) when H_2S mixed with (a) Na_2S (b) H_2O (c) 0.1 M NaOH (d) 1 M NaOH (Jang et al., 2006).

2008). These results showed that WI method is more efficient in the production of hydrogen.

3.4. CdS / TiO_2 (Nanotubes) composite photocatalyst for hydrogen production

Nanotubes (NTs) of titanate is used for the systemization of CdS/TiO_2 composite with changing diameters by a simple method of ion change and sulfurization process followed at moderate temperature. Using this composite as a photocatalyst increased the production of hydrogen (H_2). In this process, almost 43.4% yield was obtained under the visible region around the wavelength of 525 nm. High efficiency might be obtained due to these reasons (1) The effects of synergetic among TiO_2 NTs and nanoparticles (NP) of CdS (2) Another major role of homogeneous distribution of CdS particle and quantum effect.

In this photocatalytic hydrogen production process following reactions occur

$$CdSNP/TiO_2NT + hv \rightarrow CdSNP(h^+)/TiO_2NT(e^-)$$

$$TiO_2NT(2e^-) + 2H_2O \rightarrow H_2 + 2OH^-$$

$$SO_3^{-2} + 2OH^- + 2h^+ \rightarrow SO_2^- + 2H^+$$

$$S^{-2} + 2h^+ \rightarrow S$$

The production of hydrogen was recorded by using a composite of CdS (NP)/ TiO_2 (NTs) with time efficiency like for the first NT CdSNT-1, for the second used after 4 h denoted as CdSNT-2, physical mixture and neat powder of CdS. The average hydrogen (H_2) evolution during the whole process is shown in Fig. 14.

3.5. Elucidating the factors affecting hydrogen production activity using a CdS/TiO_2

The photocatalytic efficiency of the CdS/TiO_2 composite was observed by factors of hydrogen overvoltage, transfer of an electron, substrate adsorption, and cocatalyst effect. In CdS/TiO_2 composite transfer of electron play an effective role in the recombination rate of electron-hole pair. It could be more effective when a co-catalyst like Pt is used and increased the reducing and oxidizing capacity of generated electron-hole pair which makes the photocatalysis process more efficient. For this purpose, it is important to choose a catalyst carefully that matched the required output and is designed as well. The design used for elucidating factors is shown in Fig. 15 (Nagakawa and Nagata, 2021).

The above discussion shows that CdS/TiO_2 composite photocatalyst is important for the production of hydrogen. The CdS/TiO_2 have been reported by using various methods, materials, and shapes, under different experimental conditions, and the efficiency of hydrogen production is shown in Table 2.

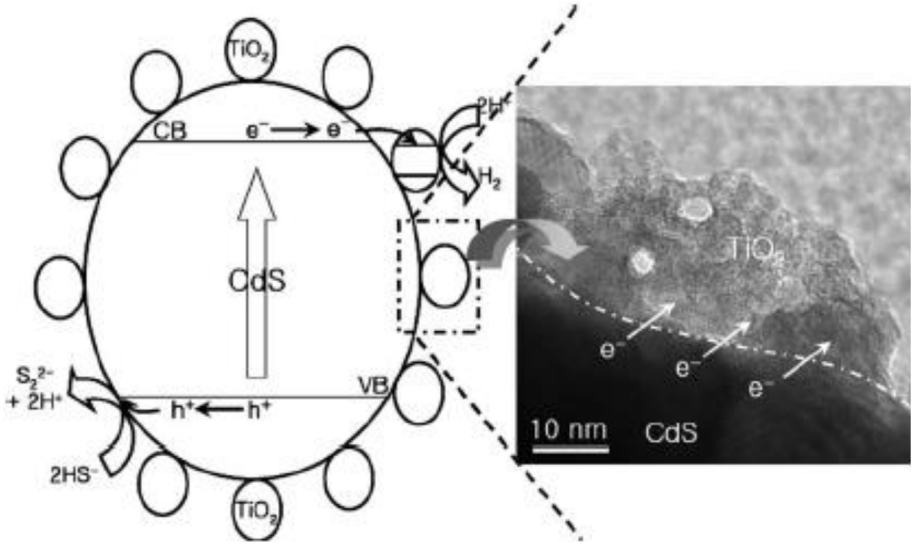

Fig. 11 Hydrogen production mechanism for CdS bulk with nano sized TiO_2 composite from H_2S (Jang et al., 2006).

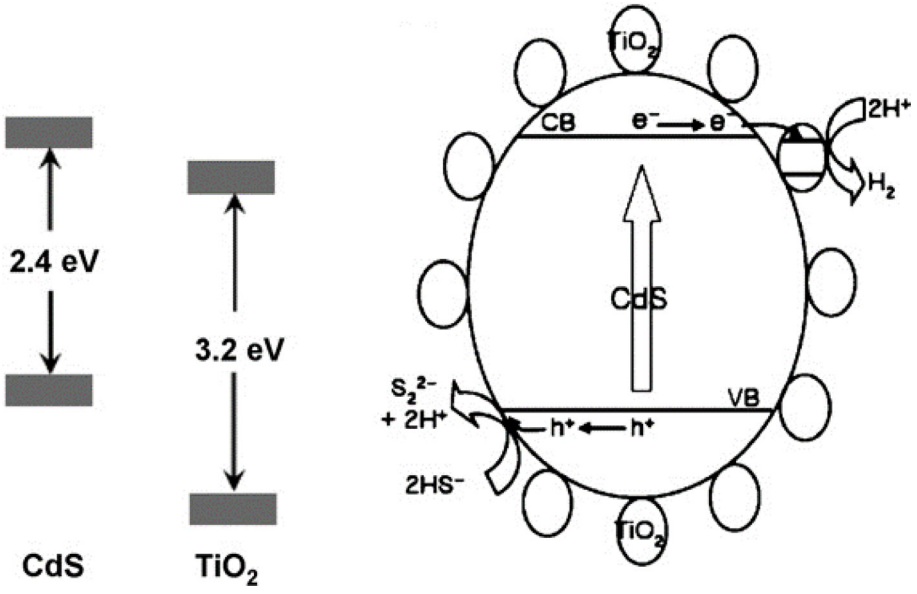

Fig. 12 Hydrogen (H_2) production model for CdS bulk with nano-sized TiO_2 composite from H_2S in presence of 0.1 M Na_2S + 0.02 M Na_2SO_3 (Jang et al., 2007a).

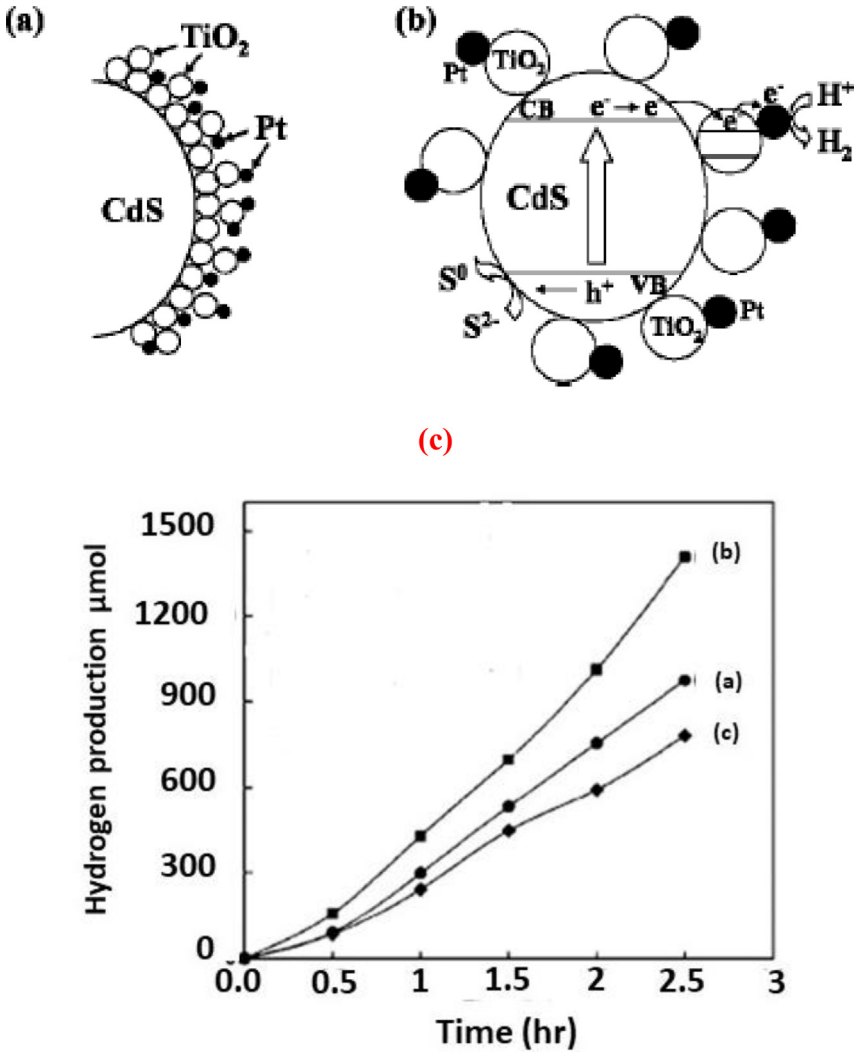

Fig. 13 (a) Operational mechanism of composite with CdS/TiO_2 in the presence of catalyst Pt (b) Activity model of CdS/TiO_2 composite in the presence of catalyst Pt (c) Rate of hydrogen production in time (hr) (Jang et al., 2008).

4. WO_3/g C_3N_4 composite photocatalyst for hydrogen production

Graphitic Carbon Nitride (g C_3N_4) polymeric semiconductor recently has gained the attention of researchers because of its great efficiency in photocatalysis activity, g C_3N_4 polymer inorganic coupling with Z scheme nanocomposite of semiconductor behaves as an efficient photocatalyst in the irradiation of visible light (Ge et al., 2012, Su et al., 2022, Tian et al., 2015, Lang et al., 2015).

WO_3 also gains attention due to its narrow band gap activated in visible light but WO_3 is not suitable for single electron O_2 reduction in the conduction band due to low photooxidation ability. The researcher tried their best to overcome these limits of WO_3 such as deposition of noble metal, controlling of size, and many other coupling phenomena but still no satisfactory result was obtained. g C_3N_4 also gains attain due to its activation in the visible region and favorable in the reduction as conduction band minimum −1.12 ev which makes it to best for the production of hydrogen(Chen et al., 2014b). But is a limitation in photocatalytic efficiency in that its electron-hole pair of recombination is too fast. Many strategies adopted to overcome this limitation such as controlling size and coupling with some other semiconductors were most favorable (Cheng et al., 2017, Han et al., 2018, Kim et al., 2022, Bi and Xu, 2011).

g C_3N_4 and WO_3 due to narrow semiconductors driven by visible light within the solar spectrum. In this regard composites of WO_3/g C_3N_4 became the center of interest due to their high efficiency in photocatalytic reaction for the production of hydrogen. Photocatalyst Composites of WO_3/g C_3N_4 has been investigated for the production of hydrogen by using different techniques of preparation, different shape or size (nanocomposite, nanotubes, nanosheets, bulk, and others), different dimensions (1D,2D,3D) and different scheme (Z and S) (Chen et al., 2014b, Fu et al., 2019a, Cui et al., 2017, Kim et al., 2022, Zhou et al., 2022).

In this domain of composite of WO_3/g C_3N_4 photocatalyst for hydrogen production there are hundreds of researches article published as shown in Fig. 16.

4.1. Composite WO_3/g C_3N_4 with a different mass content of WO_3

The phase structure, the separation efficiency of electron-hole pair, optical adsorption, and absorption are key factors involved in the photocatalytic activity of any substance. The composite of WO_3/g C_3N_4 formed by using a calcination process with variation in mass % of WO_3 (6.1 %,9.7 %, and 16.6 %) with a specific value of g C_3N_4. The photocatalytic activity efficiency was observed by the degradation of methyl blue. The photocatalyst properties by using different techniques. WO_3 and g C_3N_4 not altered their structure crystal phase after hybridization as shown in XRD pattern Fig. 17 (Huang et al., 2013a).

The comparison between pure WO_3, g-C_3N_4, and their composite showed that the composite is more efficient for photocatalytic activity as compared to pure one. Further analysis shows that 16.6% WO_3 quantity has produced more sites for photocatalytic reactivity. Because the surface increased with an increase in % of WO_3 quantity which provides a favorable position for the diffusion of products and adsorption of reactants. Its increased efficiency of photocatalytic reactivity (Kang et al., 2012, Dong et al., 2013, Sun et al., 2012, Tersoff, 1984).

The above discussion has showed that visible range absorption and adsorption enhancement key point for an increase in photocatalytic activity. But there is another important effect involved in the efficiency of photocatalytic activity which is charge separation. The separation of electrons and holes de-

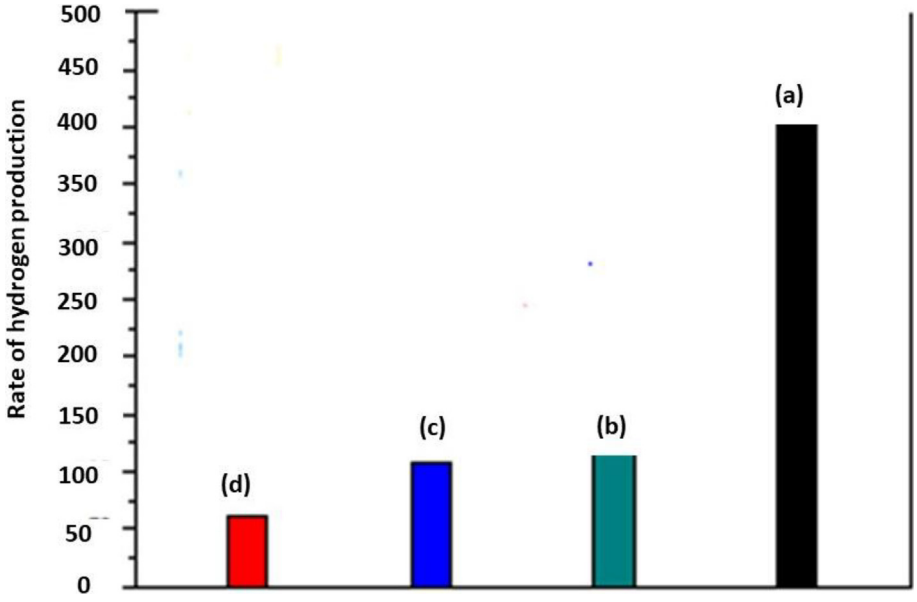

Fig. 14 The average hydrogen production by using (a) CdSNT-1 (b) CdSNT-2 (c) Physical mixture 20% CdS + 80% TiO_2 (d) neat powder of CdS (Li et al., 2010).

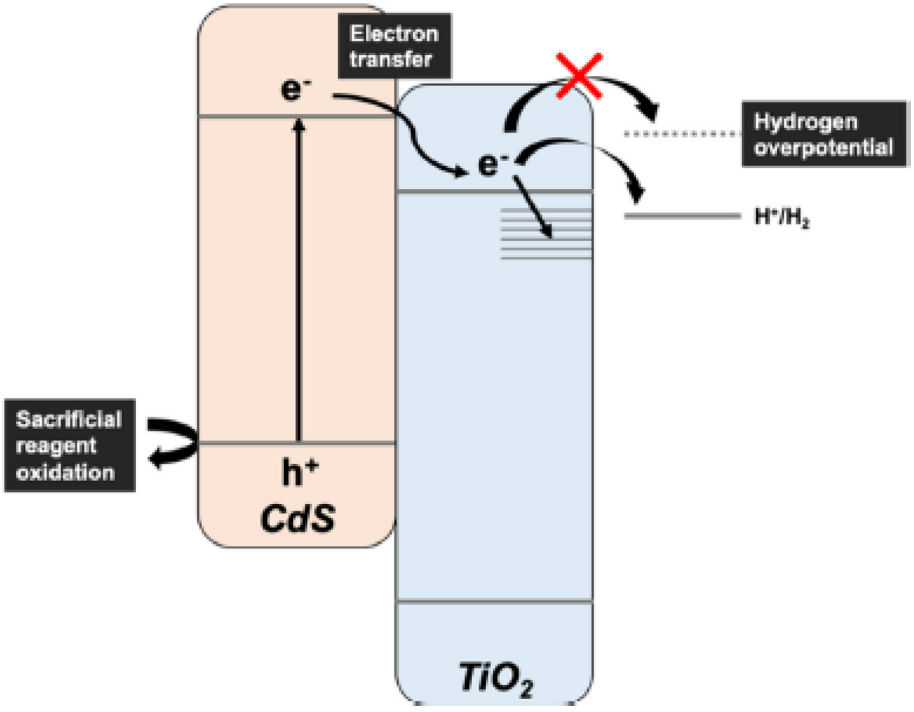

Fig. 15 Hydrogen production mechanism CdS/ TiO_2 by using reducing agent (Nagakawa and Nagata, 2021).

Table 2 CdS/ TiO_2 composite reported by researcher.

Material	Experimental condition	Production rate of hydrogen	Ref
CdS/TiO_2 nanocomposite with $TiCl_4$	Variation in use of catalyst from mole ratio 0,0.2,0.5,0.8 and 1.	1.6 mol/cm^2	(Guan et al., 2004)
TiO_2 nanotubes Pt/ CdS	Catalyst with aqueous solution 300 W (W) Xe lamp wavelength > 400 nm from water	402umolh^{-1}	(Li et al., 2010)
Pt/TiO_2 / CdS zeolite Y	Catalyst 50 g aqueous solution 200 W Xe lamp 320 < wavelength < 570 nm from water	12 umolh^{-1}	(White and Dutta, 2011)
CdS/TiO_2 nano bulk	Catalyst 0.1 g Aqueous solution 500 W Hg lamp wavelength > 420 nm from H_2S	980umolh^{-1}	(Jang et al., 2006)
TiO_2 / CdS	Catalyst 0.08 g Aqueous solution 500 W Hg lamp wavelength > 420 nm	72% after 6 h	(Huo et al., 2011)
TiO_2 nanotubes/ CdS	Catalyst 25 mg aqueous solution 200 W Halogen lamp 420 < wavelength < 800 nm	91.6% after 2 h	(Zhou et al., 2011)
TiO_2 / CdS/ cross-linked chitosan	Catalyst 50 mg with aqueous solution 300 W Xe lamp wavelength > 400 nm	37.4% after 5 h (visible)	(Zhu et al., 2013)
Pt/TiO_2 / CdS	aqueous solution 400 W Xe lamp monochromatic (470 nm) radiation	0.21 μmol min^{-1}	(Strataki et al., 2010)
TiO_2 / CdS graphene	Catalyst 50 m × 75 mm film 8 W LED lamp	33% after 2.5 h	(Park et al., 2013)
Nanowires TiO_2 / CdS film	4-*tert*-butyl pyridine (0.125 M) in 3-meth- oxy propio nitrile,and 1-vinyl-3-methyl imidazolium iodide (0.70 M),LiI(0.1 M),I2 (40 mM), 300 W Xe lamp	16.4 % after 1 h	(Lee et al., 2009)
TiO_2 / CdS/Pt	Reducing agent MeOH with effecting factor overvoltage and electron transfer	459.5 umolh^{-1}	(Nagakawa and Nagata, 2021)
Ti_3CN@TiO_2 / CdS	nanoflower morphology from water splitting	3393.4 μmol$g^{-1}h^{-1}$	(Li et al., 2022)

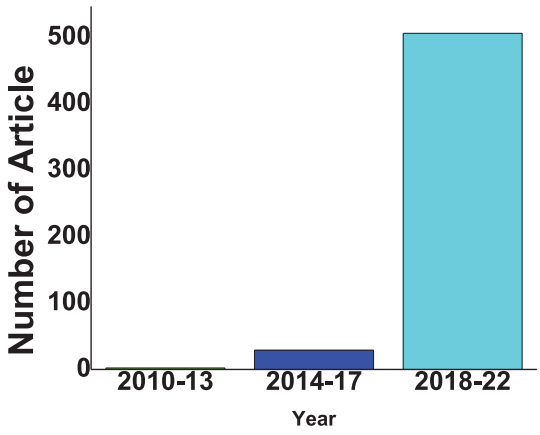

Fig. 16 No of Publication on WO_3/g C_3N_4 composite photocatalyst for hydrogen production with the gap of 4 years from 2010 to 2022 from google scholar (Scholar, 2023).

pends on the band edge position of two semiconductors, as band structure is accountable for the efficient separation and generation of charge carriers. The proper direction of the band structure is useful in the creation of interface depletion of charge carriers (Alferov, 1998, Yan et al., 2010c).

The possible mechanism involved in this process has shown in Fig. 18. The bottom of the valence band of WO_3 has 3.43 eV and the conduction band 0.75 eV energy. The g-C_3N_4 has the valence band (VB) bottom 1.57 eV and conduction band (CB) −1.13 eV energy. The band gap of WO_3 has 3.43-0.75 = 2.6 8 eV and g-C_3N_4 1.57- (-1.13) = 2.70 eV energy. This shows that both semiconductor irradiation under visible light creates electron-hole pairs. Its shows that the potential of the g-C_3N_4 CB edge is less than the WO_3, which means the g-C_3N_4 electrons in the excitation state directly insert into the WO_3 CB. In the same way, the VB of g-C_3N_4 is less than the WO_3. So, holes are transfer from WO_3 to g-C_3N_4. The distribution of electrons is on one side of the junction and holes on another side of the junction increased the separation time of the electron and hole pair which has increased the photocatalytic activity of the composite. This is clear that the composite of g-C_3N_4/WO_3 has a higher efficiency as compared to the pure g-C_3N_4 and WO_3 (Chakraborty et al., 2012, Cui et al., 2017).

The degradation efficiency of the substance is calculated by using the formula

$$E = (1 - C/C_o)x100 = (1 - A/A_o) \times 100$$

Here A_o and A are corresponding absorption values of concentration of a substance at initial C_o and concentration after some time (t) C (Xing et al., 2019).

g-C_3N_4/WO_3 composite has a greater value of substance degradation as compared to the pure g-C_3N_4 and WO_3 due to its higher efficiency in photocatalytic activity and Composite g-C_3N_4/WO_3 enhanced due to the enhanced absorption and electron-hole pair separation(Cui et al., 2017).

The p hotocatalytic activity of g-C_3N_4/WO_3 composite increased as the WO_3 % content increased until 25% after that the photocatalytic activity decreased so maximum photocatalytic activity achieved in g-C_3N_4/WO_3 composite as 25% content of WO_3 as shown in Fig. 19 (Han et al., 2018).

Change in different properties like surface area and band gap energy with different mass content % shown in Table 3 (Cui et al., 2017).

In the same way when methanol was used and activity of hydrogen production rate was observed every half hour of WO_3/g-C_3N_4 composite prepared under the Z-Scheme. It provides the maximum hydrogen production of 224.4 umol/h with 25% WO_3 content as shown in Fig. 20 (Cui et al., 2017).

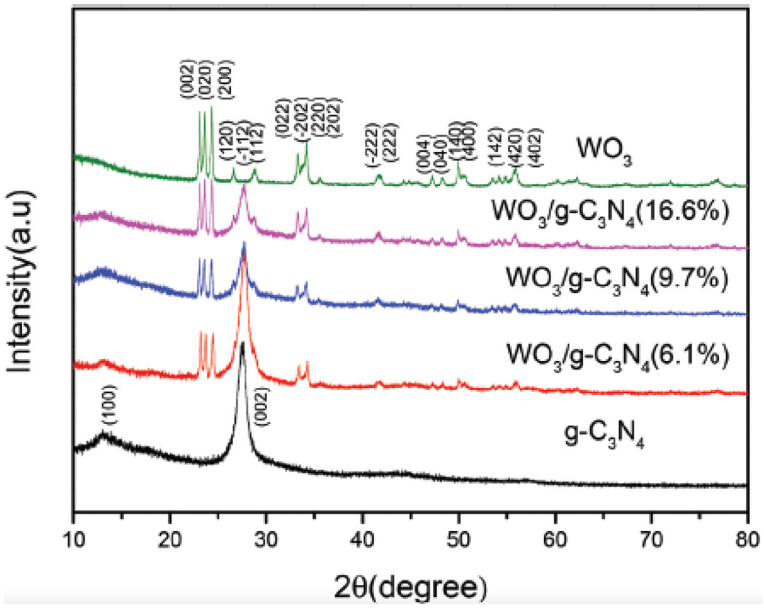

Fig. 17 XRD pattern of WO_3,g-C_3N_4 and composite of WO_3/g-C_3N_4 with variation in percentage of WO_3 6.1%, 9.7% and 16.6% (Zhang et al., 2012).

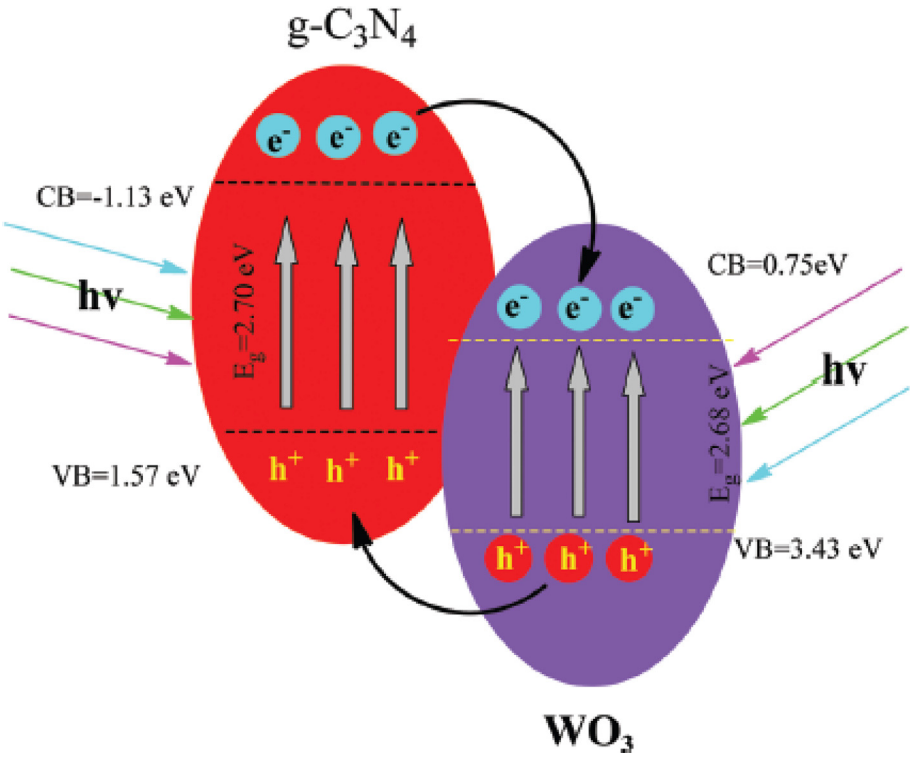

Fig. 18 Photocatalytic mechanism of g-C_3N_4/WO_3 composites under irradiation of visible light (Xing et al., 2019).

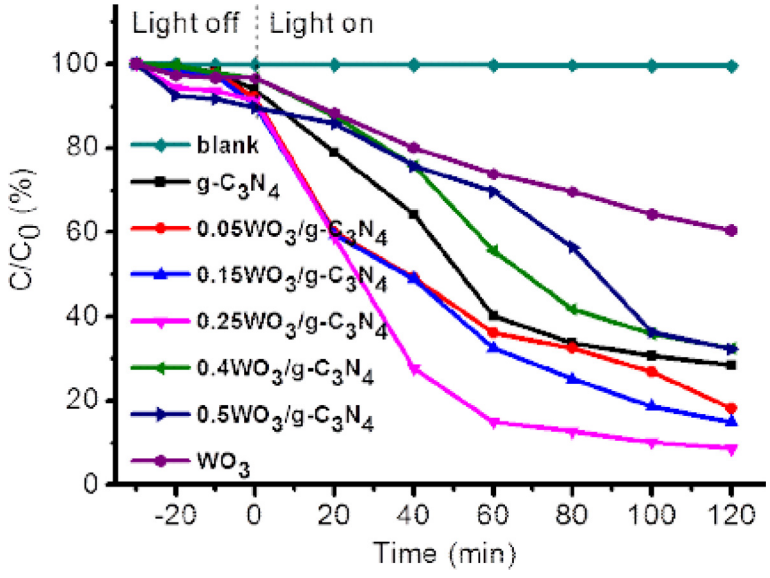

Fig. 19 Shows degradation activity under light irradiation with different mass % content of WO_3 at 0, 0.05, 0.15,0.25,0.4,0.5 in g-C_3N_4/ WO_3 composite and without light (Yan et al., 2010b).

4.2. Two-dimensional (2D) composite of g-C_3N_4/WO_3 photocatalytic activity for hydrogen production

The 2D g-C_3N_4/WO_3 composite was prepared by using the cost-effective and simple method of hydrothermal. The production of hydrogen was observed under the irradiation of visible light. During the process of the hydrothermal composite formed by using nanoparticles (NP) of WO_3 attached uniformly with g-C_3N_4 nanosheets (NS). This was observed in orthorhombic shape NP grain size 5 nm-80 nm of WO_3 attached uniformly with NS of g-C_3N_4. The synthesis process of the composite is shown in Fig. 21 (Han et al., 2018, Yan et al., 2010a).

Table 3 Shows the change in surface area and band gap with different % of WO_3.

WO_3 % in g-C_3N_4/WO_3	Surface area (m^2/g)	Energy (eV)
5%	68.1	2.57
15%	84.6	2.62
25%	100.6	2.73
35%	75	2.54
40%	72.7	2.52
50%	70.5	2.4

The Schematic shows that WO_3 dissolved hexadecyl trimethyl ammonium bromide (CTAB) and stirred for 12 h, g-C_3N_4 also stirred for 12 h, and then both mixed and stirred for 24 h at a temperature of 240 °C. After this calcination of the composite was done almost for 3 h at a temperature of 450 °C. in this way 2D composite of WO_3/g-C_3N_4 was prepared(Wang et al., 2016).

Then 2D g-C_3N_4/WO_3 was used for the hydrogen production and the whole experiment was conducted in the evacuation and closed gas circulation system. The water circulation is used to keep the temperature of the system at room temperature. The photocatalytic powder of 100 mg is suspended in aqueous triethanolamine (TEOA). The co-catalyst of Pt was directly deposited on the photocatalyst and irradiation started after 15 min vacuum. The concentration of H_2 was collected after every hour and analyzed in a chromatograph (Huang et al., 2013a, Yi et al., 2017).

The morphology of the composite showed that it has a layered structure which caused to increase in the surface area as an increase in the surface area increased the active sites for photocatalytic activity. In the same way, its enhanced absorption of visible light generates more electron-hole pairs. The 2D structure of the composite is also helpful in enhancing the separation of electron hole-pair. The co-catalyst of Pt was further used to enhance the photocatalytic activity of the composite for the hydrogen evolution from the water. As the Pt has high metallic characteristics the electrons in CB of g-C_3N_4 combine with H^+ and produced H_2 and holes in WO_3 VB oxidized the molecule of TEOA. In this process, Z-Scheme is used for hydrogen production. Z- Scheme slows down the process of recombination of an electron from CB to combine with a hole from the VB. As the recombination rate increased the photocatalytic activity of the composite increased in the production of hydrogen. In this way, Z-Scheme plays an important role in increasing the efficiency of photocatalyst composite. The mechanism is shown in Fig. 22 (Xu et al., 2018, Guan et al., 2017, Nie et al., 2018).

The highest generation rate of H_2 was observed at 1853 m-mol/h by using a composite of 2D g-C_3N_4/WO_3 which was almost 6.5 times as compared to g-C_3N_4 NS. The WO_3 synergistic effect and nano architectures effect of the g-C_3N_4 plays a vital role in the performance of their 2D composite in the production of hydrogen. The Z-Scheme not only increased the separation time of the electron-hole it also increased the surface area which creates more active sites. All these factors make a more efficient 2D composite of WO_3/g-C_3N_4 (Liu et al., 2016).

4.3. 2D/2D composite of WO_3/g-C_3N_4 for production of hydrogen

To improve the photocatalytic activity of WO_3/g-C_3N_4 composite 2D structure of both WO_3 and g-C_3N_4 used for preparation and step (S) scheme used. The 2D/2D design of surface–surface contact increased the surface area which developed more active sites and increased photocatalytic activity efficiency. For the fabrication of 2D/2D structure, the ultrathin nanosheet of WO_3 and g-C_3N_4 sized ranged from 2.5 nm to 3.5 nm used. WO_3 /g-C_3N_4 composites were prepared by using self-assembly electrostatic nanosheets of WO_3 and g-C_3N_4 as shown in Fig. 23 (Zhang et al., 2020).

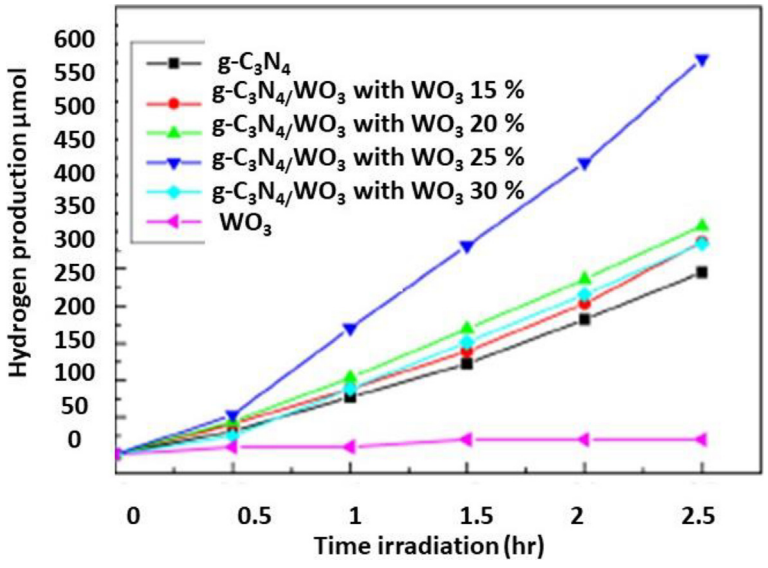

Fig. 20 Hydrogen production rate for WO_3, g-C_3N_4 and WO3/g-C_3N_4 composite with time irradiation (Xing et al., 2019).

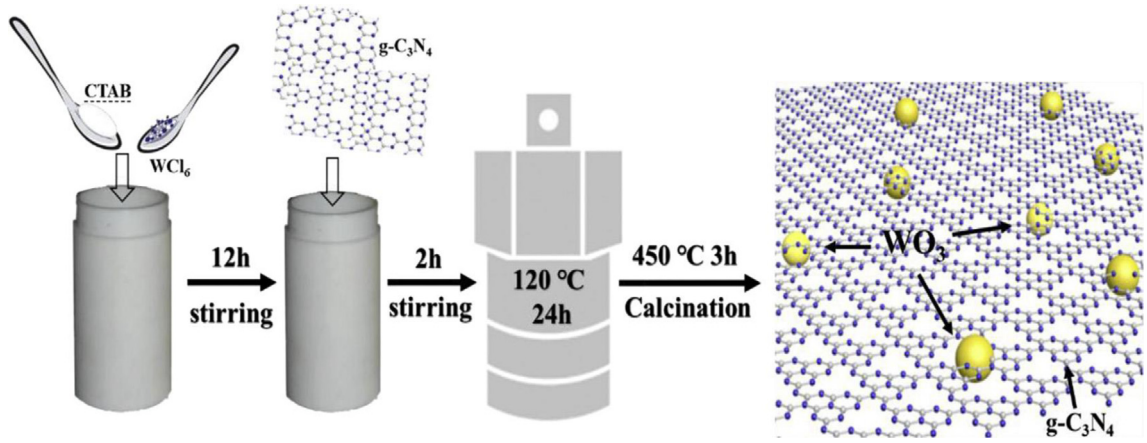

Fig. 21 Schematic of preparation of 2D g-C_3N_4/WO_3 composite by using hydrothermal method stirring for 12 h of WO_3,g-C_3N_4 for 2 h and calcination at 450 °C for 3 h (Ge et al., 2013).

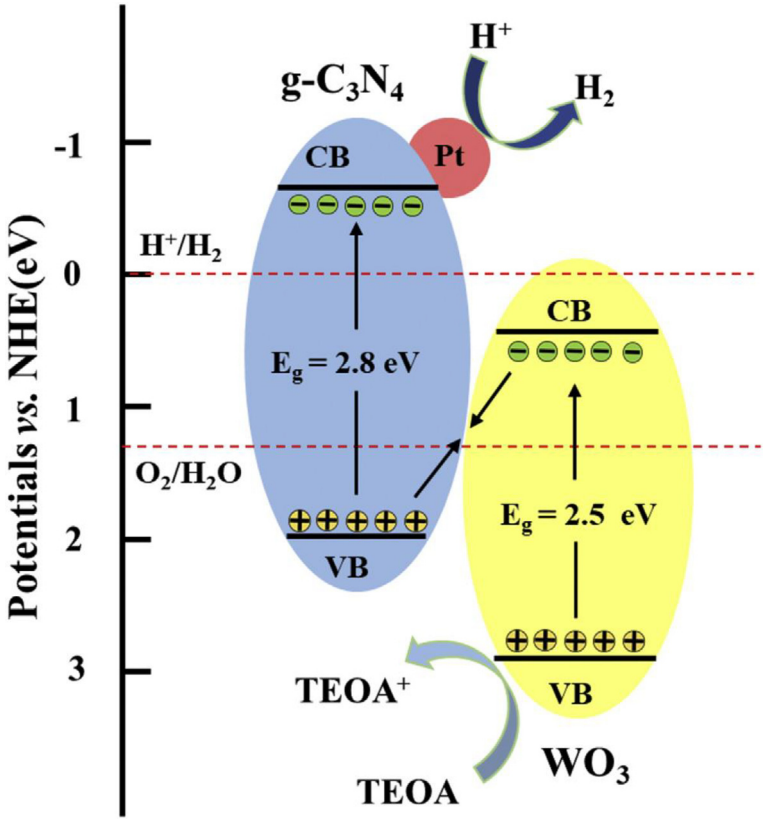

Fig. 22 Mechanism of 2D g-C_3N_4/WO_3 composite for hydrogen production (Fu et al., 2019b).

Then this composite was used for the production of hydrogen with a co-catalyst of Pt. the mechanism used for the hydrogen production was S Scheme for this composite. The whole mechanism is shown in Fig. 24 (Zhang et al., 2020).

In the S-Scheme WO_3 was used as oxidation due to a lower Fermi level and g-C_3N_4 reduction to a larger fermi level but when both are in close contact fermi level became the same. As WO_3 accepts electrons from the g-C_3N_4 an electric field induces at the interface. The band edge of WO_3 moves downward due to the acceptance of electrons and g-C_3N_4 upward due to the transfer of electrons. So, when the light falls on composite electron transfer from both VB to CB. In this way, coulomb interaction between charges, edge bending, and internal field increased the recombination of some electron-hole pairs but at the same time increased the separation of some electron-hole pairs. The inactive electron holes are eliminated by using S-Scheme but it holds the active electron-hole pair. This process provides the 2D/2D WO_3/g-

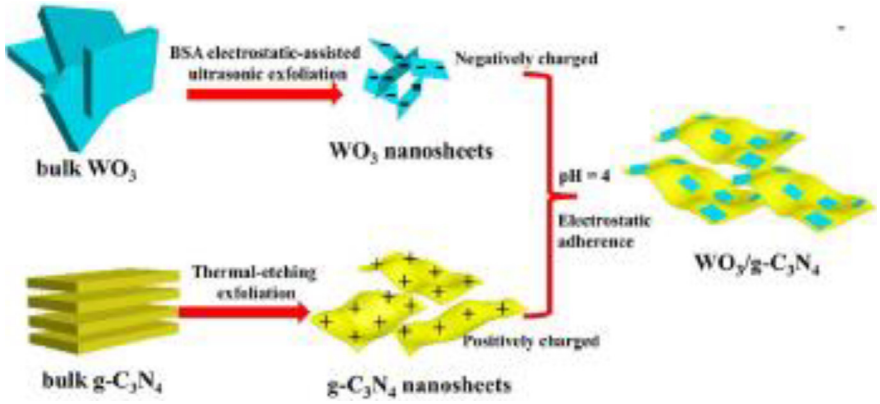

Fig. 23 Schematic of 2D/2D WO_3 /g-C_3N_4 composites preparation (Zhang et al., 2020).

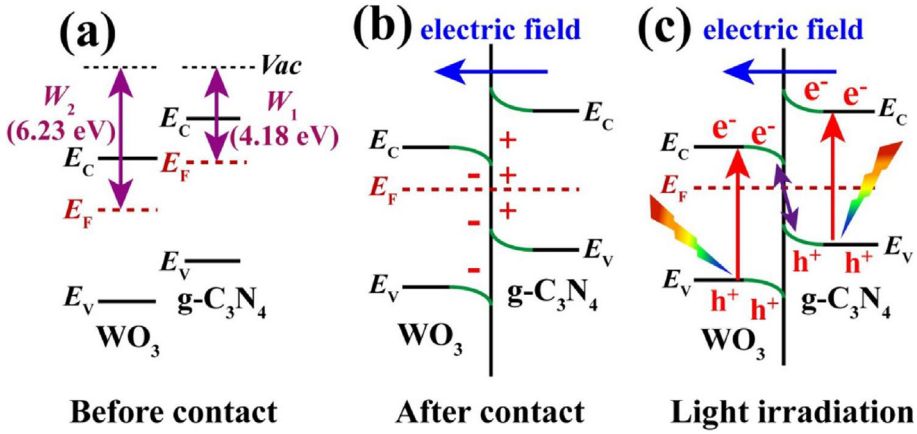

Fig. 24 Schematic of mechanism of WO_3 and g-C_3N_4 (a) before contact (b) after contact and (c) light irradiation by using S scheme charge transfer (Byskov et al., 2000a).

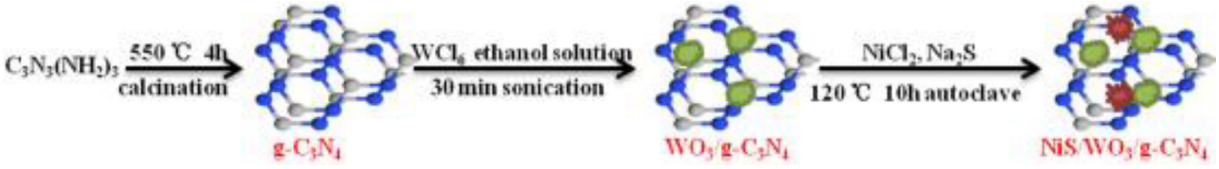

Fig. 25 Schematic of NiS-assisted WO_3/g-C_3N_4 composite for 4 h at 550 °C temperature, 30 min sonication and autoclaves for 10 h 120 °C temperature (Zhang et al., 2020).

C_3N_4 composite strong force for photocatalytic activity in the splitting of water for the production of hydrogen (Liu et al., 2017, Yang et al., 2018).

The above discussion shows that S scheme 2D/2D WO_3/g-C_3N_4 composite is more efficient as compared to pure WO_3 and g-C_3N_4 for the production of hydrogen. The mechanism involved in this process is interesting as it eliminates useless electron-hole pairs in photocatalytic activity and holds useful electron-hole from VB and CB (Xu et al., 2017b).

4.4. WO_3/g-C_3N_4 composite performance enhanced by using nickel sulfide (NiS) for hydrogen production

Already being discussed composite is better than pure or doped semiconductor for photocatalytic efficiency. But the composite efficiency also increased by using different co-catalysts. The NiS directly involved in the composite of WO_3/g-C_3N_4 increased its efficiency 8.9 times of pure g-C_3N_4

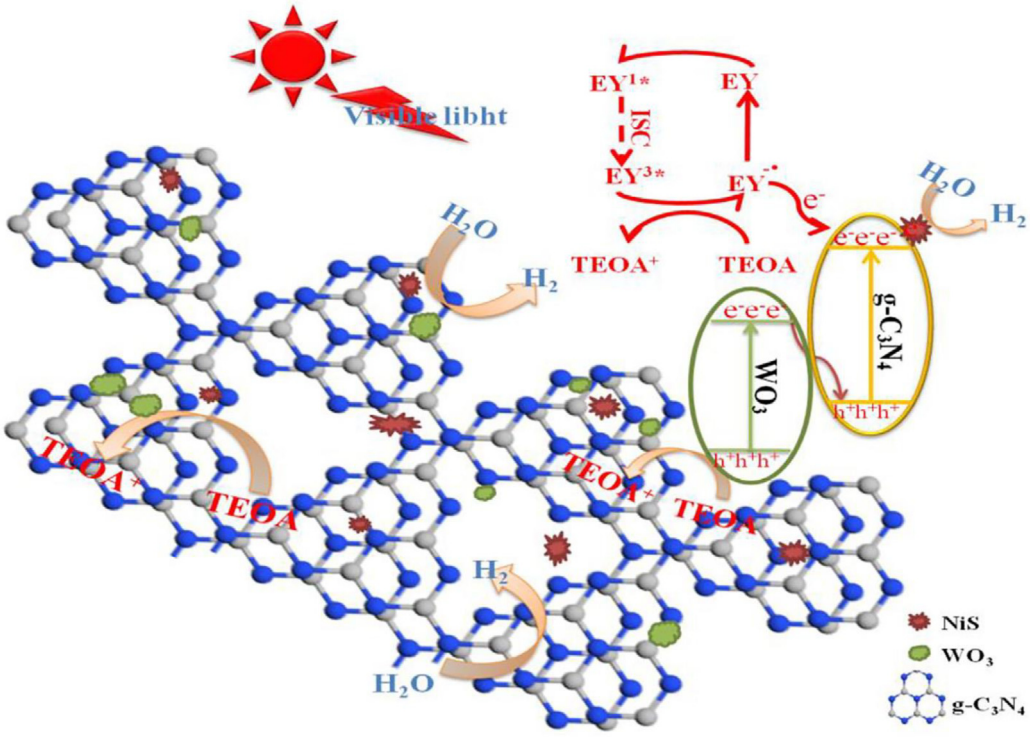

Fig. 26 Schematic mechanism of WO_3/g-C_3N_4 composite assisted with NiS for the hydrogen production (Zhang et al., 2020).

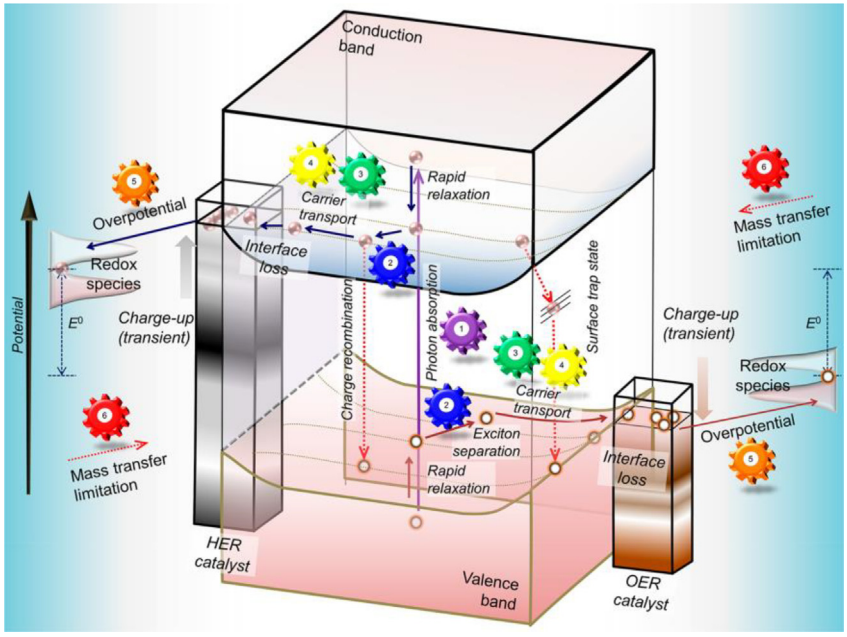

Fig. 27 Mechanism of water splitting shows first mass transfer then light fall on it and oxidation reduction occur (Takanabe, 2017).

previously it was reported 6.5 times. The in-situ growth of NiS on the WO_3 modifies the composite of WO_3/g-C_3N_4 because it enhances surface area which provides more active sites for the production of hydrogen by using photocatalytic activity (Zhang et al., 2020).

The sample was prepared through the hydrothermal method and NiS plays the role of catalyst in this process which increased active sites for photocatalytic reaction in VB and CB. The synthesis procedure is shown in Fig. 25 (Zhang et al., 2020).

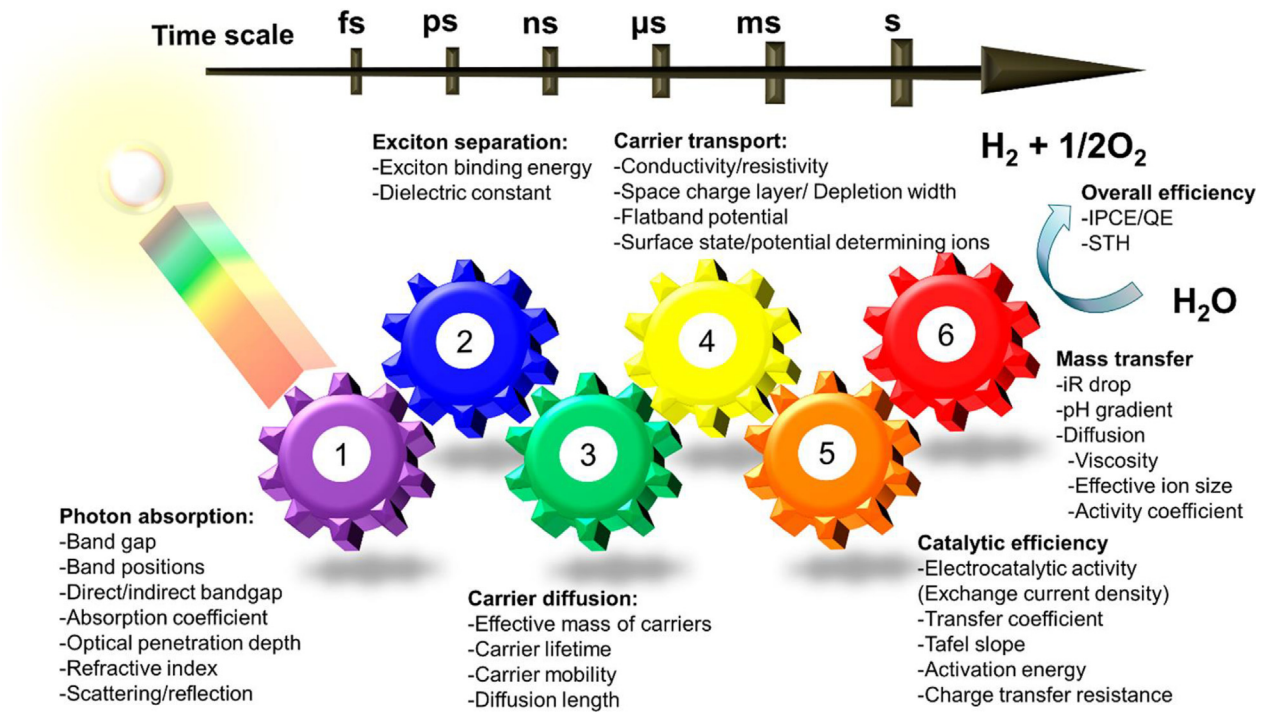

Fig. 28 Parameters affect the production of hydrogen through water splitting involves Carrier transport, Excitation separation, Photon absorption, Carrier diffusion, Catalytic efficiency and Mass transfer (Takanabe, 2017).

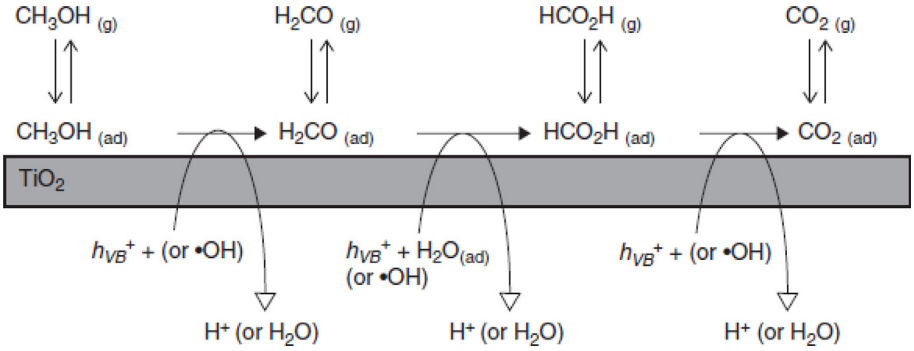

Fig. 29 Schematic for Hydrogen Production through Organic Compound (Chiarello and Selli, 2014).

The mechanism involved in this process shows when light irradiation on the sample the electron-hole pair is generated in the WO_3/g-C_3N_4 composite. The NiS behave as a cocatalyst which accelerates the charge carrier in the g-C_3N_4 CB which drives the production of hydrogen increased and at the same time, holes in VB of WO_3 oxidized strongly with the TEOA. NiS also promotes an electron from the oxidation of TEOA which increased active sites for the production of hydrogen. In this way, the production rate of hydrogen was enhanced significantly by involving NiS in composite and boosted its photocatalytic efficiency. The mechanism is shown in Fig. 26 (Zhang et al., 2020, Chen et al., 2014a, Byskov et al., 2000b, Liu et al., 2017, Yang et al., 2018, Xu et al., 2017c, Xu et al., 2017a).

In this process maximum hydrogen production rate of 2929.1 umol/gh was observed and it involved two factors one surface area increased and the second time of separation electron-hole pair increased (Zhang et al., 2020).

All the above discussion shows composites of Cds/TiO_2 and WO_3/g-C_3N_4 increased the efficiency of hydrogen production through photocatalytic activity. The researchers are using these composites for hydrogen production from water splitting and air. The basic principle of hydrogen production through water splitting and organic compound by using schemes like Z and S used involved in the composite is briefly discussed below discussion.

5. Hydrogen production as renewable energy resource using photocatalyst

The production of hydrogen becomes of huge interest to the researcher as it needs an hour to find renewable energy re-

source which must be environmentally friendly and the method of photocatalyst best compare to another method as it is low cost and involve visible region irradiation. Hydrogen fuel is the future of the world. First the production of hydrogen from water splitting important topic of discussion for the researcher (Di et al., 2019, Xu et al., 2020a, Fajrina and Tahir, 2019, Konn et al., 2015).

5.1. Hydrogen production by water splitting

The basic concept in the production of hydrogen through water splitting involves a semiconductor. When a semiconductor material dissolves in water and light fall on it then an electron is generated in the CB which react with the positive ion of hydrogen and produce hydrogen on the contrary hole in VB react with the negative hydroxyl ion of water and form oxygen. This is the basic photocatalytic concept of water splitting and the production of hydrogen. The whole process involved in hydrogen production is shown in Fig. 27 (Takanabe, 2017).

The main parameters involved in which efficiency of hydrogen production through water splitting are photon absorption, carrier diffusion, catalytic efficiency, mass transfer, carrier transport, and excitation separation. As more photon is absorbed the more electron-hole more generated which increased photocatalytic activity. In the same way, when there are more active sites, the carrier diffuses and excites the water molecule and split to produce hydrogen. The separation of charge carriers also plays an important role as electron-hole pairs separate for a long time they will reduce and oxidize water molecules at a large scale.in this way large quantity of hydrogen is produced. The parameter involved in this process is shown in the schematic of Fig. 28 (Takanabe, 2017).

5.2. Hydrogen production by using organic compound

Another famous and used method for hydrogen production use of the organic compound as organic compound combined with VB holes efficiently and used as sacrificial agents for the production of hydrogen. The organic compound uses a different mechanism as compared to water splitting. There are two main steps involved in this mechanism:

1. Direct capture of hole.
2. Indirectly as free radicals of hydroxide attacked.

The using of an organic compound like methanol for hydrogen production involves the following reaction takes place.

$$H_2O + 2hv^{+}H^{+} + 2OH^{\cdot}$$

$$CH_3OH + 2OH^{\cdot}H_2CO + 2H^{+}$$

$$H_2CO + 2OH^{\cdot}HCO_2H + 2H^{+}$$

$$HCO_2H + 2OH^{\cdot}CO_2 + 2H^{+}$$

$$2H^{+} + 2e^{-}H_2$$

The electron from CB is involved in the reduction of proton for the production of hydrogen given by photo-oxidation of methanol. The whole mechanism is shown in schematic Fig. 29 (Chiarello and Selli, 2014).

The production rate of hydrogen in this process depends upon the optical, and electrical characteristics and surface area of an organic compound.

6. Schemes involved in photocatalytic activity of composites for hydrogen production

There are two main schemes involved in the production of hydrogen through photocatalytic activity. First is Z Scheme and other S Schemes.

6.1. Z Scheme

The Z Scheme idea was first discussed by A.J. Bard for photocatalysts. In Z Scheme observed in composites of two semiconductors. One act as oxidized and the second as a reduced agent the electron-hole pair generated when light fall on it. Then photogenerated electron from CB reacts with the acceptor and creates a donor (Bard, 1979, Low et al., 2017, Madhusudan et al., 2021).

$$Acceptor + e^{-}donor$$

And photogenerated holes in VB react with the donor and form the acceptor.

$$donor + h^{+}Acceptor$$

In this way, the electron-hole pair reacted with the substance in the presence of light. This is the simplest concept to understand the Z Scheme. The Schematic of the direct Z Scheme shown in Fig. 30 used in composite used for serval purposes and one of the important purposes for the production of hydrogen (Yuan et al., 2017, Liu et al., 2018).

6.2. S Scheme

The Z Scheme has several limitations (1) confined to the phase of the solution (2) Side reactions involved (3) pH sensitivity and (4) light shielding.

To prevent all these limitations researchers introduced a new S Scheme. The S Scheme is involved in a composite of two semiconductors. Two generalized semiconductors are OP with lower work functions as compared to RP. The following S Scheme steps are involved for their photocatalytic activity. (1) When semiconductors are closed in contact RP electrons diffuse in OP, which creates a depletion layer of electrons on the interface of RP and OP. Thus, RP charged positively and OP negatively. The internal electric field induced in RP and OP accelerates the electrons to RP from OP. (2) When two semiconductors RP and OP come in close contact they are aligned at the same level. As the fermi level of OP aligned upward and RP downward. So, bending in the band urges the recombination of CB electrons of OP with VB holes of RP. (3)

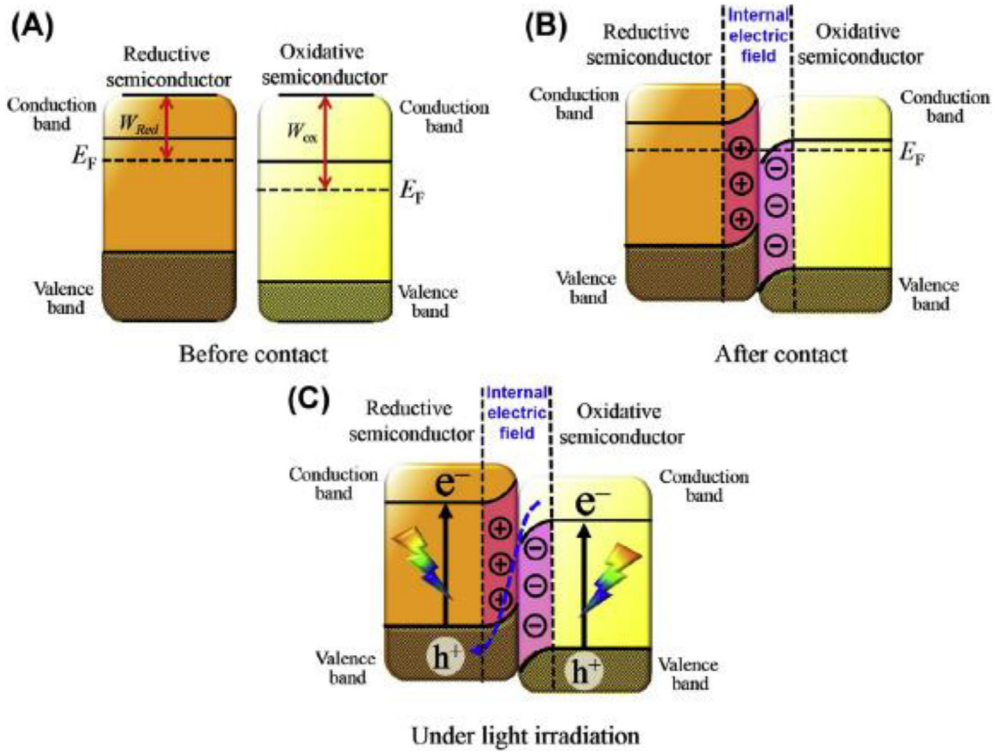

Fig. 30 Schematic of Z Scheme (A) Before Contact no change in fermi energy(B) After Contact change in fermi energy (C) Under light Irradiation creates band edge (Low et al., 2020).

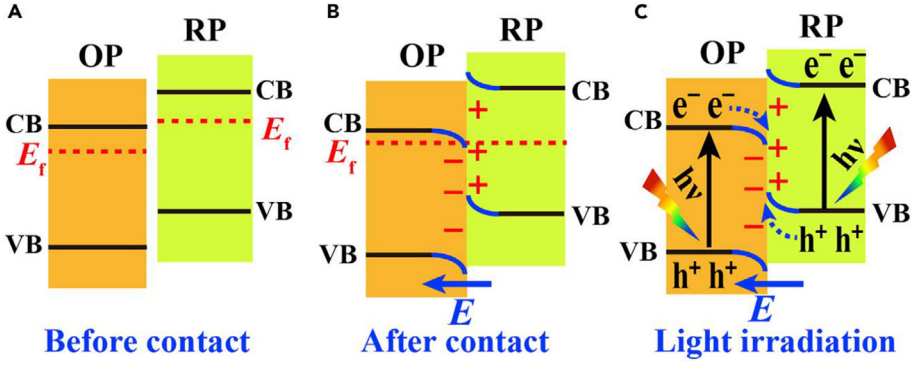

Fig. 31 Schematic of S scheme for two general semiconductor OP and RP (A) Before contact (B) After Contact (C) Under light Irradiation (Xu et al., 2020b).

The electron-hole pair recombined at the interface due to the Coulomb force. On the whole useless electron-hole pair is eliminated by recombination and useable powerful electron-hole pair holds for photocatalytic activity. The whole mechanism involved in this process is shown in the Fig. 31 (Yang et al., 2018).

In the S Scheme, there are three main factors involved which act as driven forces band bending, electric force, and Coulombic attraction. This is a useful scheme in the production of hydrogen by using composites for Photocatalytic activity.

7. Conclusion

The production of hydrogen through the photocatalytic activity of composites becomes a great area of interest through water splitting and using organic compounds. As hydrogen production is one of the best fuels to fulfill the energy requirement in the future. This review elaborates on the different CdS/TiO_2 and g-C_3N_4/WO_3 composites under different conditions for the photocatalytic activity used for the production of hydrogen. This showed the efficiency of hydrogen production is limited due to different characteristics of semiconductors like fast recombination rate and instability. Therefore, researchers fo-

cused to develop a new design for these composites to increase their photocatalytic efficiency. These limitations are reduced by using the co-catalyst, different schemes S and Z, and 2D structure of composite material. Among Schemes, S is best to increase the efficiency of the photocatalytic activity of composites. The 2D structure composites are more efficient in photocatalytic activity and produced a large rate of hydrogen as 2D structure increased active sites for the electron-hole pair which increased the efficiency of photocatalytic activity of composite. Hence, among all 2D composites are best for photocatalytic activity. Moreover, the production of hydrogen through photocatalytic activity and its use as fuel to fight with energy crisis are the top priority of the world as it is environmentally friendly and cost-effective.

8. Future prospective

The future prospective of these composites' that researchers will study 2D structure of composites with the assistance of the co-catalysts by using the S Scheme and this work will be laid the foundation for hydrogen production as fuel on an industrial scale.

Declaration of Competing Interest

The authors declare that they have no known competing financial interests or personal relationships that could have appeared to influence the work reported in this paper.

Acknowledgments

The authors express their gratitude to the Deanship of Scientific Research at King Khalid University for funding this work through the Small Research Group Project under grant number RGP.2-122-43. Princess Nourah bint Abdulrahman University Researchers Supporting Project number (PNURSP2023R55), Princess Nourah bint Abdulrahman University, Riyadh, Saudi Arabia. This study is supported via funding from Prince Sattam bin Abdulaziz University project number (PSAU/2023/R/1444).

Conflict of Interest

It is certified that there is no conflict of interest regarding the material discussed in this manuscript.

References

Ajma, Z., Ul Haq, M., Naciri, Y., Djellabi, R., Hassan, N., Zaman, S., Murtaza, A., Kumar, A., Al-Sehemi, A.G., Algarni, H.J.C., 2022. Recent advancement in conjugated polymers based photocatalytic technology for air pollutants abatement: Cases of CO2, NOx, and VOCs. Chemosphere 136358.

Akpan, U.G., Hameed, B.H., 2009. Parameters affecting the photocatalytic degradation of dyes using TiO2-based photocatalysts: A review. J. Hazard. Mater. 170, 520–529.

Alferov, Z.I.J.S., 1998. The history and future of semiconductor heterostructures. Semiconductors 32, 1–14.

An, X., Jimmy, C.Y., 2011. Graphene-based photocatalytic composites. Rsc Adv. 1, 1426–1434.

Anpo, M., Yamashita, H., Ichihashi, Y., Fujii, Y., Honda, M., 1997. Photocatalytic reduction of CO2 with H2O on titanium oxides anchored within micropores of zeolites: effects of the structure of the active sites and the addition of Pt. J. Phys. Chem. B 101, 2632–2636.

Bard, A.J., 1979. Photoelectrochemistry and heterogeneous photocatalysis at semiconductors. J. Photochem. 10, 59–75.

Bi, D., Xu, Y., 2011. Improved photocatalytic activity of WO3 through clustered Fe2O3 for organic degradation in the presence of H2O2. Langmuir 27, 9359–9366.

Byskov, L.S., Nørskov, J.K., Clausen, B.S., Topsøe, H.J.C.L., 2000a. Edge termination of MoS 2 and CoMoS catalyst particles. Catal. Lett. 64, 95–99.

Chakraborty, A.K., Kebede, M.A.J.R.K.Mechanisms & catalysis, 2012. Preparation and characterization of WO 3/Bi 3 O 4 Cl nanocomposite and its photocatalytic behavior under visible light irradiation. React. Kinet. Mech. Catal. 106, 83–98.

Chen, D., Cheng, Y., Zhou, N., Chen, P., Wang, Y., Li, K., Huo, S., Cheng, P., Peng, P., Zhang, R., 2020. Photocatalytic degradation of organic pollutants using TiO2-based photocatalysts: A review. J. Clean. Prod. 268, 121725.

Chen, S., Hu, Y., Meng, S., Fu, X., 2014b. Study on the separation mechanisms of photogenerated electrons and holes for composite photocatalysts g-C3N4-WO3. Appl. Catal. B 150, 564–573.

Chen, J., Shen, S., Guo, P., Wang, M., Wu, P., Wang, X., Guo, L., 2014a. In-situ reduction synthesis of nano-sized Cu2O particles modifying g-C3N4 for enhanced photocatalytic hydrogen production. Appl. Catal. B 152, 335–341.

Cheng, C., Shi, J., Hu, Y., Guo, L.J.N., 2017. WO3/g-C3N4 composites: one-pot preparation and enhanced photocatalytic H2 production under visible-light irradiation. Nanotechnology 28, 164002.

Cheng, L., Xiang, Q., Liao, Y., Zhang, H.J.E., Science, E., 2018. CdS-based photocatalysts. Energ. Environ. Sci. 11, 1362–1391.

Chiarello, G. & Selli, E. 2014. Photocatalytic production of hydrogen. Advances in hydrogen production, storage and distribution. Elsevier.

Chu, S., Cui, Y., Liu, N., 2017. The path towards sustainable energy. Nat. Mater. 16, 16–22.

Cui, L., Ding, X., Wang, Y., Shi, H., Huang, L., Zuo, Y., Kang, S.J. A.S.S., 2017. Facile preparation of Z-scheme WO3/g-C3N4 composite photocatalyst with enhanced photocatalytic performance under visible light. Appl. Surf. Sci. 391, 202–210.

Di, T., Xu, Q., Ho, W., Tang, H., Xiang, Q., Yu, J.J.C., 2019. Review on metal sulphide-based Z-scheme photocatalysts. ChemCatChem 11, 1394–1411.

Dong, F., Zhao, Z., Xiong, T., Ni, Z., Zhang, W., Sun, Y., Ho, W.-K. Interfaces, 2013. In situ construction of g-C3N4/g-C3N4 metal-free heterojunction for enhanced visible-light photocatalysis. ACS Appl. Mater. Interfaces 5, 11392–11401.

Doubi, Y., Hartiti, B., Siadat, M., Labrim, H., Fadili, S., Tahri, M., Thevenin, P.J.C.R.Technology, 2022. The high impact of solution flow rate on optical properties of TiO_2 thin layers for optoelectronic applications. Cryst. Res. Technol. 2200129

Dutta, V., Sharma, S., Raizada, P., Thakur, V.K., Khan, A.A.P., Saini, V., Asiri, A.M., Singh, P., 2021. An overview on WO3 based photocatalyst for environmental remediation. J. Environ. Chem. Eng. 9, 105018.

Elmaci, G., Frey, C.E., Kurz, P., Zümreoğlu-Karan, B., 2016. Water oxidation catalysis by using nano-manganese ferrite supported 1D-(tunnelled), 2D-(layered) and 3D-(spinel) manganese oxides. J. Mater. Chem. A 4, 8812–8821.

Elmaci, G., Ertürk, A.S., Sevim, M., Metin, Ö., 2019. MnO2 nanowires anchored on mesoporous graphitic carbon nitride (MnO2@ mpg-C3N4) as a highly efficient electrocatalyst for the oxygen evolution reaction. Int. J. Hydrogen Energy 44, 17995–18006.

Elmaci, G.K., Frey, C.E., Kurz, P., Zumreoglu-Karan, B.J.I.C., 2015. Water oxidation catalysis by birnessite@ iron oxide core–shell nanocomposites. Inorg. Chem. 54, 2734–2741.

Elmaci, G., Özgenç, G., Kurz, P., Zumreoglu-Karan, B.J.S.E., Fuels, 2020. Enhanced water oxidation performances of birnessite and

magnetic birnessite nanocomposites by transition metal ion doping. Sustain. Energy Fuels 4, 3157–3166.
Fajrina, N., Tahir, M., 2019. A critical review in strategies to improve photocatalytic water splitting towards hydrogen production. Int. J. Hydrogen Energy 44, 540–577.
Fu, J., Xu, Q., Low, J., Jiang, C., Yu, J., 2019a. Ultrathin 2D/2D WO3/g-C3N4 step-scheme H2-production photocatalyst. Appl. Catal. B 243, 556–565.
Ge, L., Zuo, F., Liu, J., Ma, Q., Wang, C., Sun, D., Bartels, L., Feng, P., 2012. Synthesis and efficient visible light photocatalytic hydrogen evolution of polymeric g-C3N4 coupled with CdS quantum dots. J. Phys. Chem. C 116, 13708–13714.
Ge, L., Han, C., Xiao, X., Guo, L., 2013. Synthesis and characterization of composite visible light active photocatalysts MoS2–g-C3N4 with enhanced hydrogen evolution activity. Int. J. Hydrogen Energy 38, 6960–6969.
Ghouri, M., Ahmed, E., Ali, A., Ramzan, M., Irfan, M., 2021. Improved photocatalytic H2 evolution over composites based on niobium pentoxide, metal sulfides and graphene. Mater. Sci. Semicond. Process. 122, 105492.
Guan, G., Kida, T., Kusakabe, K., Kimura, K., Fang, X., Ma, T., Abe, E., Yoshida, A., 2004. Photocatalytic H2 evolution under visible light irradiation on CdS/ETS-4 composite. Chem. Phys. Lett. 385, 319–322.
Guan, G., Xia, J., Liu, S., Cheng, Y., Bai, S., Tee, S.Y., Zhang, Y.W., Han, M.Y.J.A.M., 2017. Electrostatic-driven exfoliation and hybridization of 2D nanomaterials. Adv. Mater. 29, 1700326.
Han, X., Xu, D., An, L., Hou, C., Li, Y., Zhang, Q., Wang, H., 2018. WO3/g-C3N4 two-dimensional composites for visible-light driven photocatalytic hydrogen production. Int. J. Hydrogen Energy 43, 4845–4855.
Hermesmann, M., Müller, T., 2022. Green, turquoise, blue, or grey? environmentally friendly hydrogen production in transforming energy systems. Prog. Energy Combust. Sci. 90, 100996.
Hu, J., Liu, A., Jin, H., Ma, D., Yin, D., Ling, P., Wang, S., Lin, Z., Wang, J., 2015. A versatile strategy for shish-kebab-like multi-heterostructured chalcogenides and enhanced photocatalytic hydrogen evolution. J. Am. Chem. Soc. 137, 11004–11010.
Huang, R., Wu, J., Zhang, M., Liu, B., Zheng, Z., Luo, D.J.M. Design, 2021. Strategies to enhance photocatalytic activity of graphite carbon nitride-based photocatalysts. Mater. Des. 210, 110040.
Huang, L., Xu, H., Li, Y., Li, H., Cheng, X., Xia, J., Xu, Y., Cai, G.J. D.T., 2013a. Visible-light-induced WO 3/gC 3 N 4 composites with enhanced photocatalytic activity. Dalton Trans. 42, 8606–8616.
Huo, Y., Yang, X., Zhu, J., Li, H., 2011. Highly active and stable CdS–TiO2 visible photocatalyst prepared by in situ sulfurization under supercritical conditions. Appl. Catal. B 106, 69–75.
Husseina, M., Mohammedb, K., Talibc, R.J.C.L., 2022. Energy band gaps and optical absorption properties of the CdZns and CdZns: PEO thin films prepared by chemical bath deposition. Chalcogenide Lett. 19, 329–335.
Janaky, C., de Tacconi, N.R., Chanmanee, W., Rajeshwar, K., 2012. Bringing conjugated polymers and oxide nanoarchitectures into intimate contact: Light-induced electrodeposition of polypyrrole and polyaniline on nanoporous WO3 or TiO2 nanotube array. J. Phys. Chem. C 116, 19145–19155.
Jang, J.S., Li, W., Oh, S.H., Lee, J.S., 2006. Fabrication of CdS/TiO2 nano-bulk composite photocatalysts for hydrogen production from aqueous H2S solution under visible light. Chem. Phys. Lett. 425, 278–282.
Jang, J.S., Ji, S.M., Bae, S.W., Son, H.C., Lee, J.S., 2007a. Optimization of CdS/TiO2 nano-bulk composite photocatalysts for hydrogen production from Na2S/Na2SO3 aqueous electrolyte solution under visible light ($\lambda \geq$ 420 nm). J. Photochem. Photobiol. A Chem. 188, 112–119.
Jang, J.S., Kim, H.G., Borse, P.H., Lee, J.S., 2007b. Simultaneous hydrogen production and decomposition of H2S dissolved in alkaline water over CdS–TiO2 composite photocatalysts under visible light irradiation. Int. J. Hydrogen Energy 32, 4786–4791.
Jang, J.S., Choi, S.H., Kim, H.G., Lee, J.S., 2008. Location and state of Pt in platinized CdS/TiO2 photocatalysts for hydrogen production from water under visible light. J. Phys. Chem. C 112, 17200–17205.
Jiang, Z., Qian, K., Zhu, C., Sun, H., Wan, W., Xie, J., Li, H., Wong, P.K., Yuan, S., 2017. Carbon nitride coupled with CdS-TiO2 nanodots as 2D/0D ternary composite with enhanced photocatalytic H2 evolution: a novel efficient three-level electron transfer process. Appl. Catal. B 210, 194–204.
Kang, H.W., Lim, S.N., Song, D., Park, S.B., 2012. Organic-inorganic composite of g-C3N4–SrTiO3: Rh photocatalyst for improved H2 evolution under visible light irradiation. Int. J. Hydrogen Energy 37, 11602–11610.
Khatamian, M., Saket Oskoui, M., Haghighi, M., Darbandi, M., 2014. Visible-light response photocatalytic water splitting over CdS/TiO2 and CdS–TiO2/metalosilicate composites. Int. J. Energy Res. 38, 1712–1726.
Kim, B., Jung, Y., Park, B.J., Das, G., Yoon, H.H., Yoon, Y.S., 2022. Photo-assisted electrolysis of urea using Ni-modified WO3/g-C3N4 as a bifunctional catalyst. Int. J. Hydrogen Energy 47, 5797–5806.
Konn, C., Charlou, J.-L., Holm, N.G., Mousis, O.J.A., 2015. The production of methane, hydrogen, and organic compounds in ultramafic-hosted hydrothermal vents of the Mid-Atlantic Ridge. Astrobiology 15, 381–399.
Lang, J., Liu, M., Su, Y., Yan, L., Wang, X., 2015. Fabrication of the heterostructured CsTaWO6/Au/g-C3N4 hybrid photocatalyst with enhanced performance of photocatalytic hydrogen production from water. Appl. Surf. Sci. 358, 252–260.
Lee, J.S., 2005. Photocatalytic water splitting under visible light with particulate semiconductor catalysts. Catal. Surv. Asia 9, 217–227.
Lee, J.-C., Kim, T.G., Lee, W., Han, S.-H., Sung, Y.-M., 2009. Growth of CdS nanorod-coated TiO2 nanowires on conductive glass for photovoltaic applications. Cryst. Growth Des. 9, 4519–4523.
Li, D., Yang, C., Rajendran, S., Qin, J., Zhang, X., 2022. Nanoflower-like Ti3CN@ TiO2/CdS heterojunction photocatalyst for efficient photocatalytic water splitting. Int. J. Hydrogen Energy 47, 19580–19589.
Li, C., Yuan, J., Han, B., Jiang, L., Shangguan, W., 2010. TiO2 nanotubes incorporated with CdS for photocatalytic hydrogen production from splitting water under visible light irradiation. Int. J. Hydrogen Energy 35, 7073–7079.
Li, H., Zhang, L., Lu, H., Ma, J., Zhou, X., Wang, Z., Yi, C., 2020. Macro-/nanoporous Al-doped ZnO/cellulose composites based on tunable cellulose fiber sizes for enhancing photocatalytic properties. Carbohydr. Polym. 250, 116873.
Lian, Z., Xu, P., Wang, W., Zhang, D., Xiao, S., Li, X., Li, G., 2015. C60-decorated CdS/TiO2 mesoporous architectures with enhanced photostability and photocatalytic activity for H2 evolution. ACS Appl. Mater. Interfaces 7, 4533–4540.
Liao, M., Su, L., Deng, Y., Xiong, S., Tang, R., Wu, Z., Ding, C., Yang, L., Gong, D., 2021. Strategies to improve WO3-based photocatalysts for wastewater treatment: a review. J. Mater. Sci. 56, 14416–14447.
Liu, D., Jin, Z., Bi, Y.J.C.S.Technology, 2017. Charge transmission channel construction between a MOF and rGO by means of Co–Mo–S modification. Cat. Sci. Technol. 7, 4478–4488.
Liu, Y., Liang, L., Xiao, C., Hua, X., Li, Z., Pan, B., Xie, Y.J.A.E. M., 2016. Promoting photogenerated holes utilization in pore-rich WO3 ultrathin nanosheets for efficient oxygen-evolving photoanode. Adv. Energy Mater. 6, 1600437.
Liu, X., Sayed, M., Bie, C., Cheng, B., Hu, B., Yu, J., Zhang, L., 2021. Hollow CdS-based photocatalysts. J. Materiom. 7, 419–439.
Liu, Y., Zhang, H., Ke, J., Zhang, J., Tian, W., Xu, X., Duan, X., Sun, H., Tade, M.O., Wang, S., 2018. 0D (MoS2)/2D (g-C3N4)

heterojunctions in Z-scheme for enhanced photocatalytic and electrochemical hydrogen evolution. Appl. Catal. B 228, 64–74.
Low, J., Yu, J. & Jiang, C. 2020. Design and fabrication of direct Z-scheme photocatalysts. Interface Science and Technology. Elsevier.
Low, J., Jiang, C., Cheng, B., Wageh, S., Al-Ghamdi, A.A., Yu, J.J.S. M., 2017. A review of direct Z-scheme photocatalysts. Small Meth. 1, 1700080.
Luo, C., Ren, X., Dai, Z., Zhang, Y., Qi, X., Pan, C., 2017. Present perspectives of advanced characterization techniques in TiO2-based photocatalysts. ACS Appl. Mater. Interfaces 9, 23265–23286.
Madhusudan, P., Shi, R., Xiang, S., Jin, M., Chandrashekar, B.N., Wang, J., Wang, W., Peng, O., Amini, A., Cheng, C., 2021. Construction of highly efficient Z-scheme ZnxCd1-xS/Au@ g-C3N4 ternary heterojunction composite for visible-light-driven photocatalytic reduction of CO2 to solar fuel. Appl. Catal. B 282, 119600.
Mao, J.-X., Wang, J.-C., Gao, H., Shi, W., Jiang, H.-P., Hou, Y., Li, R., Zhang, W., Liu, L., 2022. S-scheme heterojunction of CuBi2O4 supported Na doped P25 for enhanced photocatalytic H2 evolution. Int. J. Hydrogen Energy 47, 8214–8223.
Montoya, J.H., Seitz, L.C., Chakthranont, P., Vojvodic, A., Jaramillo, T.F., Nørskov, J.K., 2017. Materials for solar fuels and chemicals. Nat. Mater. 16, 70–81.
Munawar, T., Nadeem, M.S., Mukhtar, F., Manzoor, S., Ashiq, M. N., Batool, S., Hasan, M., Iqbal, F., 2022. Enhanced photocatalytic, antibacterial, and electrochemical properties of CdO-based nanostructures by transition metals co-doping. Adv. Powder Technol. 33, 103451.
Nagakawa, H., Nagata, M., 2021. Elucidating the factors affecting hydrogen production activity using a CdS/TiO2 type-II composite photocatalyst. ACS Omega 6, 4395–4400.
Nasir, M.S., Yang, G., Ayub, I., Wang, S., Wang, L., Wang, X., Yan, W., Peng, S., Ramakarishna, S., 2019a. Recent development in graphitic carbon nitride based photocatalysis for hydrogen generation. Appl. Catal B 257, 117855.
Nguyen, N.T., Altomare, M., Yoo, J., Schmuki, P., 2015. Efficient photocatalytic H2 evolution: controlled dewetting–dealloying to fabricate site-selective high-activity nanoporous Au particles on highly ordered TiO2 nanotube arrays. Adv. Mater. 27, 3208–3215.
Nie, N., Zhang, L., Fu, J., Cheng, B., Yu, J.J.A.S.S., 2018. Self-assembled hierarchical direct Z-scheme g-C3N4/ZnO microspheres with enhanced photocatalytic CO2 reduction performance. Appl. Surf. Sci. 441, 12–22.
Nunes, D., Pimentel, A., Branquinho, R., Fortunato, E., Martins, R. J.C., 2021. Metal oxide-based photocatalytic paper: A green alternative for environmental remediation. Catalysts 11, 504.
Park, C., Kefayat, U., Vikram, N., Ghosh, T., Oh, W., Cho, K., 2013. Preparation of novel CdS-graphene/TiO2 composites with high photocatalytic activity for methylene blue dye under visible light. Bull. Mater. Sci. 36, 869–876.
So, W.-W., Kim, K.-J., Moon, S.-J., 2004. Photo-production of hydrogen over the CdS–TiO2 nano-composite particulate films treated with TiCl4. Int. J. Hydrogen Energy 29, 229–234.
Soni, V., Singh, P., Quang, H.H.P., Khan, A.A.P., Bajpai, A., van Le, Q., Thakur, V.K., Thakur, S., Nguyen, V.-H., Raizada, P.J.C., 2022. Emerging architecture titanium carbide (Ti3C2Tx) MXene based photocatalyst toward degradation of hazardous pollutants: Recent progress and perspectives. Chemosphere 133541.
Strataki, N., Antoniadou, M., Dracopoulos, V., Lianos, P., 2010. Visible-light photocatalytic hydrogen production from ethanol–water mixtures using a Pt–CdS–TiO2 photocatalyst. Catal. Today 151, 53–57.
Su, F., Wang, Z., Xie, H., Zhang, Y., Ding, C., Ye, L., 2022. Structural distortion of g-C3N4 induced by N-defects for enhanced photocatalytic hydrogen evolution. Catalysts 12, 1496.
Sudhaik, A., Raizada, P., Rangabhashiyam, S., Singh, A., Nguyen, V.-H., van Le, Q., Khan, A.A.P., Hu, C., Huang, C.-W., Ahamad, T.J.S.Interfaces, 2022. Copper sulfides based photocatalysts for degradation of environmental pollution hazards: A review on the recent catalyst design concepts and future perspectives. Surfaces and Interfaces, 102182.
Sun, J.-X., Yuan, Y.-P., Qiu, L.-G., Jiang, X., Xie, A.-J., Shen, Y.-H., Zhu, J.-F.-J.-D.-T., 2012. Fabrication of composite photocatalyst gC 3 N 4–ZnO and enhancement of photocatalytic activity under visible light. Dalton Trans. 41, 6756–6763.
Takanabe, K.J.A.C., 2017. Photocatalytic water splitting: quantitative approaches toward photocatalyst by design. ACS Catal. 7, 8006–8022.
Tersoff, J.J.P.R.B., 1984. Theory of semiconductor heterojunctions: The role of quantum dipoles. Phys. Rev. B 30, 4874.
Tian, N., Huang, H., Zhang, Y., 2015. Mixed-calcination synthesis of CdWO4/g-C3N4 heterojunction with enhanced visible-light-driven photocatalytic activity. Appl. Surf. Sci. 358, 343–349.
Wang, X., Maeda, K., Thomas, A., Takanabe, K., Xin, G., Carlsson, J.M., Domen, K., Antonietti, M., 2009. A metal-free polymeric photocatalyst for hydrogen production from water under visible light. Nat. Mater. 8, 76–80.
Wang, X.-J., Tian, X., Li, F.-T., Li, Y.-P., Zhao, J., Hao, Y.-J., Liu, Y., 2016. Synchronous surface hydroxylation and porous modification of g-C3N4 for enhanced photocatalytic H2 evolution efficiency. Int. J. Hydrogen Energy 41, 3888–3895.
Wang, Q., Zhu, S., Zhao, S., Li, C., Wang, R., Cao, D., Liu, G.J.F., 2022. Construction of Bi-assisted modified CdS/TiO2 nanotube arrays with ternary S-scheme heterojunction for photocatalytic wastewater treatment and hydrogen production. Fuel 322, 124163.
Wen, J., Xie, J., Chen, X., Li, X., 2017. A review on g-C3N4-based photocatalysts. Appl. Surf. Sci. 391, 72–123.
Weng, B., Xu, Y.-J., 2015. What if the electrical conductivity of graphene is significantly deteriorated for the graphene–semiconductor composite-based photocatalysis? ACS Appl. Mater. Interfaces 7, 27948–27958.
White, J.C., Dutta, P.K., 2011. Assembly of nanoparticles in zeolite Y for the photocatalytic generation of hydrogen from water. J. Phys. Chem. C 115, 2938–2947.
Xing, P., Zhou, F., Li, Z.J.A.P.A., 2019. Preparation of WO 3/gC 3 N 4 composites with enhanced photocatalytic hydrogen production performance. Appl. Phys. A 125, 1–7.
Xu, Q., Cheng, B., Yu, J., Liu, G.J.C., 2017a. Making co-condensed amorphous carbon/g-C3N4 composites with improved visible-light photocatalytic H2-production performance using Pt as cocatalyst. Carbon 118, 241–249.
Xu, Q., Jiang, C., Cheng, B., Yu, J.J.D.T., 2017b. Enhanced visible-light photocatalytic H 2-generation activity of carbon/gC 3 N 4 nanocomposites prepared by two-step thermal treatment. Dalton Trans. 46, 10611–10619.
Xu, Q., Zhu, B., Jiang, C., Cheng, B., Yu, J.J.S.R., 2018. Constructing 2D/2D Fe2O3/g-C3N4 direct Z-scheme photocatalysts with enhanced H2 generation performance. Solar Rrl 2, 1800006.
Xu, Q., Zhang, L., Cheng, B., Fan, J., Yu, J.J.C., 2020a. S-scheme heterojunction photocatalyst. Chem 6, 1543–1559.
Yan, S., Lv, S., Li, Z., Zou, Z.J.D.T., 2010c. Organic–inorganic composite photocatalyst of gC 3 N 4 and TaON with improved visible light photocatalytic activities. Dalton Trans. 39, 1488–1491.
Yan, A., Xie, C., Zeng, D., Cai, S., Li, H.J.J.O.A., 2010a. Compounds, Synthesis, formation mechanism and illuminated sensing properties of 3D WO3 nanowall. J. Alloy. Compd. 495, 88–92.
Yang, H., Jin, Z., Hu, H., Bi, Y., Lu, G.J.A.S.S., 2018. Ni-Mo-S nanoparticles modified graphitic C3N4 for efficient hydrogen evolution. Appl. Surf. Sci. 427, 587–597.
Yang, K., Yang, Z., Zhang, C., Gu, Y., Wei, J., Li, Z., Ma, C., Yang, X., Song, K., Li, Y., 2021. Recent advances in CdS-based photocatalysts for CO2 photocatalytic conversion. Chem. Eng. J. 418, 129344.
Yi, S.-S., Yan, J.-M., Wulan, B.-R., Li, S.-J., Liu, K.-H., Jiang, Q., 2017. Noble-metal-free cobalt phosphide modified carbon nitride:

an efficient photocatalyst for hydrogen generation. Appl Catal B 200, 477–483.
Younis, S.A., Kwon, E.E., Qasim, M., Kim, K.-H., Kim, T., Kukkar, D., Dou, X., Ali, I.J.P.I.E., Science, C., 2020. Metal-organic framework as a photocatalyst: Progress in modulation strategies and environmental/energy applications. Prog. Energy Combust. Sci. 81, 100870.
Yuan, Q., Liu, D., Zhang, N., Ye, W., Ju, H., Shi, L., Long, R., Zhu, J., Xiong, Y.J.A.C., 2017. Noble-metal-free janus-like structures by cation exchange for Z-Scheme photocatalytic water splitting under broadband light irradiation. Angew. Chem. 129, 4270–4274.
Zhang, L., Hao, X., Li, Y., Jin, Z.J.A.S.S., 2020. Performance of WO3/g-C3N4 heterojunction composite boosting with NiS for photocatalytic hydrogen evolution. Appl. Surf. Sci. 499, 143862.
Zhang, J., Zhang, M., Sun, R.Q., Wang, X.J.A.C., 2012. A facile band alignment of polymeric carbon nitride semiconductors to construct isotype heterojunctions. Angew. Chem. 124, 10292–10296.
Zhou, Q., Fu, M.-L., Yuan, B.-L., Cui, H.-J., Shi, J.-W., 2011. Assembly, characterization, and photocatalytic activities of TiO2 nanotubes/CdS quantum dots nanocomposites. J. Nanopart. Res. 13, 6661–6672.
Zhou, Y., Sun, M., Yu, T., Wang, J., 2022. 3D g-C3N4/WO3/biochar/Cu2+-doped carbon spheres composites: Synthesis and visible-light-driven photocatalytic hydrogen production. Mater. Today Commun. 30, 103084.
Zhu, H., Jiang, R., Xiao, L., Liu, L., Cao, C., Zeng, G., 2013. CdS nanocrystals/TiO2/crosslinked chitosan composite: Facile preparation, characterization and adsorption-photocatalytic properties. Appl. Surf. Sci. 273, 661–669.